**BAŞKENT UNIVERSITY**
**INSTITUTE OF SCIENCE AND ENGINEERING**
**DEPARTMENT OF ELECTRICAL AND ELECTRONICS ENGINEERING**

# A CASE STUDY ON UNDERWATER COMMUNICATION BASED ON 5G TECHNOLOGY

**MASTER OF SCIENCE THESIS**

**BY**

**CEMİL MERVAN ATALAY**

**ANKARA – 2020**

**BAŞKENT UNIVERSITY**
**INSTITUTE OF SCIENCE AND ENGINEERING**
**DEPARTMENT OF ELECTRICAL AND ELECTRONICS ENGINEERING**

# A CASE STUDY ON UNDERWATER COMMUNICATION BASED ON 5G TECHNOLOGY

**MASTER OF SCIENCE THESIS**

**BY**

**CEMİL MERVAN ATALAY**

**ADVISOR**

**Murat ÜÇÜNCÜ**

**ANKARA – 2020**

**BAŞKENT UNIVERSITY**
**INSTITUTE OF SCIENCE AND ENGINEERING**

This study, which was prepared by Cemil Mervan ATALAY, for the program of Electrical and Electronics Engineering, has been approved in partial fulfillment of the requirements for the degree of Master of Science in Electrical and Electronics Engineering Department by the following committee.

Date of Thesis Defense: 19 / 08 / 2020

**Thesis Title:** A Case Study on Underwater Communicatıon Based on 5G Technology

| **Examining Committee Member** | **Signature** |
|---|---|
| Dr.Tolga NUMANOĞLU | …….. |
| Dr. Öğr. Üyesi Murat ÜÇÜNCÜ, Başkent Üniversitesi | ...…….... |
| Dr. Öğr. Üyesi Alparslan Çağrı YAPICI | …….. |

**APPROVAL**

Prof. Dr. Ömer Faruk ELALDI

Fen Bilimleri Enstitüsü Müdürü

Tarih: … /… / 2020

**BAŞKENT ÜNİVERSİTESİ**
**FEN BİLİMLER ENSTİTÜSÜ**
**YÜKSEK LİSANS / DOKTORA TEZ ÇALIŞMASI ORİJİNALLİK RAPORU**

Tarih: 04/09/ 2020

Öğrencinin Adı, Soyadı : Cemil Mervan ATALAY
Öğrencinin Numarası : 21720442
Anabilim Dalı : Elektrik-Elektronik Mühendisliği Ana Bilim Dalı
Programı : Tezli Yüksek Lisans Programı
Danışmanın Unvanı/Adı, Soyadı : Dr. Öğretim Üyesi Murat ÜÇÜNCÜ
Tez Başlığı : A Case Study on Underwater Communicatıon Based on 5G Technology

Yukarıda başlığı belirtilen Yüksek Lisans/Doktora tez çalışmamın; Giriş, Ana Bölümler ve Sonuç Bölümünden oluşan, toplam 63 sayfalık kısmına ilişkin, 04 /09/ 2020 tarihinde tez danışmanım tarafından adlı intihal tespit programından aşağıda belirtilen filtrelemeler uygulanarak alınmış olan orijinallik raporuna göre, tezimin benzerlik oranı % 6'dır.

Uygulanan filtrelemeler:

1. Kaynakça hariç
2. Alıntılar hariç
3. Beş (5) kelimeden daha az örtüşme içeren metin kısımları hariç

"Başkent Üniversitesi Enstitüleri Tez Çalışması Orijinallik Raporu Alınması ve Kullanılması Usul ve Esaslarını" inceledim ve bu uygulama esaslarında belirtilen azami benzerlik oranlarına tez çalışmamın herhangi bir intihal içermediğini; aksinin tespit edileceği muhtemel durumda doğabilecek her türlü hukuki sorumluluğu kabul ettiğimi ve yukarıda vermiş olduğum bilgilerin doğru olduğunu beyan ederim.

Öğrenci İmzası:

**APPROVAL**
…/…/2020
Advisor
Dr. Öğr. Üyesi Murat ÜÇÜNCÜ

# ACKNOWLEDGEMENTS

My deep gratitude goes first to Murat ÜÇÜNCÜ who expertly guided me through this thesis and shared the excitement for two years of the research. His unwavering wisdom kept me constantly engaged with my research.

I would like to pay my special regards to Gökhan GÜVENSEN who helped me to widen my horizon about the digital design of communication systems and who willingly shared his knowledge by teaching me the essential subjects through my research.

My appreciation also extends to TR-ARGE Company and its encouraging founder Arda SENGEC for giving me the opportunity to make research about this topic and Atıl KOPRUCU engineering director of the Company for providing me every necessary opportunity. My special thanks extends to Bahadır ERKAN whose encouragement have been valuable and also his endless enthusiasm to teach and enlighten me in many ways.

I am indebted to my Mom, who backed me up from my whole life and never beware her support from me at any point of my life. At this point, my gratitude extends to my three lovely sisters Sinem, Ayşegül and Didem who supported my education from the beginning, it is whole-heartedly appreciated that your great support proved monumental towards the success of this study.

Finally, I wish to express my deepest gratitude and love to my beloved one Melis Umay for providing me continuous encouragement throughout my research. She not only encouraged me but also involved in some parts of the research process.

This success wouldn’t have been possible without them.

## ABSTRACT

**Cemil Mervan ATALAY**

**A CASE STUDY ON UNDERWATER COMMUNICATION BASED ON 5G TECHNOLOGY**

**Baskent University Institute of Science and Engineering**

**Department Of Electrical And Electronics Engineerıng**

**2020**

Today's technology has begun to improve very fast and communication technology tries to adapt this positive change. Bigger bandwidths become a strong requirement for improved communication technology. In order to satisfy these requirements, RF 5G technology has been developed which promises a faster communication experience for end users. Faster communication not only requires bigger bandwidths but also requires a reliable and robust connection between end users. However, it is not possible to meet the new RF 5G requirements with old communication techniques since 5G aims to operate at 1 Ghz and above which brings problems as multipath, scattering due to the increase in radio frequency. Fortunately, 5G community has solved these multipath and scattering problems in the data link layer.

In underwater acoustic communication, the most challenging tasks are to recover incoming signal from multipath and scattering effects and without a state of the receiver design, it is very hard to communicate. However, we noticed that the multipath and scattering problems of RF 5G technology which arises due to the increase in frequency are the also the basic problems of Underwater communication systems. RF 5G technology has solved this problem in the data link layer by using OFDM (Orthogonal Frequency Division Multiplexing) as a modulation scheme which has started to be used with the introduction of 4G technology together with Polar Codes as forward error coding of control channel[29]. Therefore, we decided to create a state-of-the-art system that combines data link layer of RF 5G technology with best underwater acoustic (UWA) communication techniques to overcome multipath and scattering problems of UWA and we called this system Underwater 5G technology.

In this thesis, in order to construct a real time operating end to end UWA system we combined many successful telecommunication techniques of both RF and UWA

communication. This system, which is called Underwater 5G technology, is prepared on MATLAB with System Generator blocks therefore it can be directly implemented on Xilinx's FPGAs. We explained every step of the design and cleared the reasons of why the specific modules are used. In this way, the users of the system can tune the parameters according to their system performance requirements.

Underwater 5G Technology has a robust design that can establish a reliable connection at very noisy channels. As the performance criteria, the system can communicate at 7 dB SNR (Signal to Noise ratio) with very low bit error rate. These ratings are nearly hundred times better than similar works on the literature [11]. Underwater 5G technology not only better in terms of performance criteria but also it is more applicable with its easy design parameters.

**KEY WORDS:** Xilinx's FPGA, MATLAB System Generator, Underwater Communication Technology, Transmitter, Receiver, OFDM, Acoustic

**Advisor:** Dr. Öğr. Üyesi Murat ÜÇÜNCÜ, Başkent Üniversitesi, Elektrik-Elektronik Mühendisliği Bölümü

# ÖZ

**Cemil Mervan ATALAY**

**5G TEKNOLOJİSİ TEMEL ALINARAK TASARLANAN SU ALTI HABERLEŞME SİSTEMİ**

**Başkent Üniversitesi Fen Bilimleri Enstitüsü**

**Elektrik Elektronik Mühendisliği Anabilim Dalı**

**2020**

Günümüzde teknoloji çok hızlı gelişmeye başladı ve haberleşme teknolojisi bu olumlu değişime uyum sağlamaya çalışıyor. Daha büyük bant genişlikleri, gelişmiş bir haberleşme sistemi için en önemli gereksinimlerden birini oluşturmuş durumda. Bu gereksinimleri karşılamak için, son kullanıcılara daha hızlı bir haberleşme deneyimi vaat eden RF 5G teknolojisi geliştirildi. Daha hızlı iletişim yalnızca daha fazla bant genişliği gerektirmekle kalmaz, aynı zamanda son kullanıcılar arasında güvenilir ve sağlam bir bağlantı gerektirir. Ancak 5G'nin 1 Ghz ve üzerinde çalışmayı hedeflemesi, radyo frekansının artması nedeniyle kullanıcıya birden fazla sayıda ulaşma, yayılma ve saçılma gibi sorunları beraberinde getirdiği için eski iletişim teknikleriyle yeni RF 5G gereksinimlerini karşılamak mümkün değildir. Neyse ki 5G topluluğu, veri bağlantı katmanındaki bu çok yollu ve saçılma sorunlarını çözdü.

Sualtı akustik iletişiminde ise en zorlu görevler, gelen sinyali çok yollu ve saçılma etkilerinden kurtarmaktır. Kullanılan almaç tasarımında mükemmel bir mimari kurmadan, gelen verileri anlamlandırmak ve iletişim kurmak oldukça zordur. Ancak RF 5G teknolojisinin frekans artışına bağlı olarak ortaya çıkan çok yollu ve saçılma problemlerinin aynı zamanda Sualtı iletişim sistemlerinin temel problemleri olduğunu fark ettik. RF 5G teknolojisi, veri bağlantı katmanının kontrol kanalında ileri yönlü hata düzeltme algoritması olarak Polar Kodları, 4G teknolojisinin tanıtılmasıyla kullanılmaya başlanan modülasyon şeması OFDM'i (Orthogonal Frequency Division Multiplexing) ile kullanarak bu sorunu çözmüştür. Bu nedenle, Sualtı akustik kanalda meydana gelen çok yollu ve saçılma problemlerinin üstesinden gelmek için RF 5G teknolojisinin veri bağlantı katmanındaki uygulanabilir tekniklerini, en iyi su altı akustik haberleşme teknikleriyle birleştiren son teknoloji bir sistem oluşturmaya karar verdik ve bu sisteme Sualtı 5G teknolojisi adını verdik.

Bu tezde, gerçek zamanlı çalışan bir uçtan uca sualtı akustik haberleşme sistemi oluşturmak için hem kablosuz haberleşmede hem de sualtı haberleşmesinde kullanılan birçok başarılı telekomünikasyon tekniğini birleştirdik. Sualtı 5G teknolojisi olarak adlandırdığımız bu sistemi, MATLAB üzerinde System Generator blokları ile hazırlandık, bu sayede sistemimiz Xilinx'in FPGA'ları üzerinde doğrudan uygulanabilir hale geldi. Tasarımın her adımını ve kullanılan modüllerin neden kullanıldığının açıkladık. Bu şekilde, sistem kullanıcıları parametreleri sistem performans gereksinimlerine göre ayarlayabilirler.

Sualtı 5G Teknolojisi, çok gürültülü kanallarda güvenilir bir bağlantı kurabilen sağlam bir tasarıma sahiptir. Performans kriteri olarak, sistem düşük hata yapma oranıyla 7 dB Sinyal Gürültü oranı olan kanallarda iletişim kurabilir. Aynı gürültüye sahip ortamlardaki hata oranları, literatürdeki benzer çalışmalardan neredeyse yüz kat daha iyi performansa sahiptir. Sualtı 5G teknolojisi sadece performans kriterleri açısından daha iyi değil, aynı zamanda kolay tasarım parametreleri ile daha uygulanabilir bir sistem konumundadır.

**ANAHTAR SÖZCÜKLER:** Xilinx FPGA, MATLAB System Generator, Sualtı Haberleşme Teknolojisi, Verici, Almaç, OFDM, Akustik, Almaç Mimarisi

**DANIŞMAN:** Dr. Öğr. Üyesi Murat ÜÇÜNCÜ, Başkent Üniversitesi, Elektrik-Elektronik Mühendisliği Bölümü

# TABLE OF CONTENTS

# LIST OF TABELS

**Page**

# LIST OF FIGURES

**Page**

# LIST OF SYMBOLS AND ABBREVIATIONS

| | |
|---|---|
| ADC | Analog to digital converter |
| AWGN | Additive white Gaussian noise |
| BER | Bit error rate |
| BPSK | Binary phase shift keying |
| CDMA | Code division multiple access |
| CFC | Coarse frequency compensation |
| CP | Cyclic prefix |
| CSCGRV | Circularly symmetric complex Gaussian random variable |
| DAC | Digital to analog converter |
| DFT | Discrete fourier transform |
| DSP | Digital signal processing |
| $E_b/N_0$ | Bit energy to power spectral noise density ratio |
| $E_s/N_0$ | Symbol energy to power spectral noise density ratio |
| FDA | Filter design and analyzer |
| FEC | Forward error correction |
| FFC | Fine frequency compensation |
| FFT | Fast fourier transform |
| FIR | Finite impulse response |
| FPGA | Field programmable gate array |
| FSK | Frequency shift keying |
| ICI | Inter channel interference |
| IFFT | Inverse fast fourier transform |
| IP | Intellectual property |
| ISI | Inter symbol interference |
| LTE | Long term evolution |
| NF | Noise floor |
| OFDM | Orthogonal frequency division multiplexing |
| OTP | Open transport protocol |
| OWA | Open wireless architecture |
| OQPSK | Offset quadrature phase shift keying |
| PLL | Phased-locked loop |
| PSK | Phase shift keying |
| QAM | Quadrature amplitude modulation |
| QPSK | Quadrature phase shift keying |
| RF | Radio frequency |
| SC | Successive cancellation |
| SCL | Successive cancellation list |
| SNR | Signal to noise ratio |
| TDMA | Time division multiple access |
| UWA | Underwater communication |
| VHDL | Very high speed integrated circuit hardware description language |
| 1G | First generation |
| 2G | Second generation |
| 3G | Third generation |
| 4G | Fourth generation |
| 5G | Fifth generation |

# 1. INTRODUCTION

Submarines, mine-warfare, oil extraction facilitates in the oceans, monitoring systems for climate in the sea, military harbor protection facilities have increased the demand for wireless communication under the sea. Rapidly developing technology in the stated areas required more throughputs. To satisfy the demand for better communication throughput underwater, several researches have been carried out in the last 40 years.

The first problem is to determine how to propagate the information underwater. Today, there are three candidate methodologies which are stated as communication by using electromagnetic, acoustic or optical waves. Electromagnetic waves can only radiate at low frequencies and over extremely short distance (a few meters at 10 kHz) under the water [1]. Optical communication is an alternative for underwater communication. Optical signals offers high data rates (above MHz) and are best used in the blue-green region (around 500 nm) [1]. However, optical signals cannot propagate beyond 100 meters due to high attenuation problem. Therefore, wireless communication at underwater acoustic communication is considered to be superior to optical communication.

After the propagation methodologies are cleared, in the literature, state of the art telemetry techniques with high speed are discussed [2][3][4]. These researches are focused on to find a better modulation scheme for underwater communication. Important modulation schemes such as FSK, QPSK [2], PSK, QAM [3], OFDM [5] are evaluated in terms of their suitability in underwater transmission. However, underwater acoustic channel is very noisy and is not suitable to establish a stable communication due to the necessity to estimate the acoustic channel precisely. For this issue, many researches have been carried out to estimate the underwater acoustic channel [5]. Apart from the physical layer, some other researches are focused on the network layer to provide a better underwater communication [6][7][8][9].

Last research topic to decrease Bit Error Rate for underwater communication is to use a FEC (Forward Error Correction) methodology. Popular FEC methodologies such as Reed Solomon [10] and Polar Codes [11] are implemented for underwater communication systems.

Moreover, some designs in the literature focused on creating a complete receiver system which includes both modulation schemes and forward error correction methodologies. OFDM modulation and Turbo Coding combined in [25]. They reach 2.8 Kbps to 9 Kbps data rate with $10^{-4}$ Bit Error Rate.

OFDM Modulation is also combined with Polar Coding [11] and in that design $10^{-7}$ Bit Error Rate is reached at 7dB SNR however with a Polar Coding Rate of 1/4 which means 3/4 of the data consist of frozen bits and only 1/4 bits consist of message bits.

As it is clearly explained in the previous paragraphs, many modulation schemes, forward error correction methodologies, network technologies and channel estimation techniques are used to improve the underwater communication. The common point of all of these schemes is that they all are inspired from RF technology. As RF communication technology improves, underwater communication is also improved.

Although most of the known modulation schemes, FEC and channel prediction methodologies are implemented on underwater communication systems, there is not any end to end real time underwater system implementation in the literature which combines techniques to present a novel system to overcome problems such as multipath. Therefore, in this thesis, we developed a novel end to end real time under water acoustic communication system. Since this system's physical layer is inspired from RF 5G Technology, we called our system "Underwater 5G Technology".

Underwater 5G Technology is a novel underwater acoustic communication system which offers a stable point to point communication with a significant less Bit Error Rate compared to the other existing technologies. In this thesis, both the transmitter and receiver side of this technology is well designed and implemented. The digital design of all the components of transmitter and receiver are conducted by using MATLAB System Generator, implemented on Xilinx's ZYNQ-7020 FPGA and the design is tested practically by using a water tank.

This thesis is organized as five chapters. Chapter 1 is the introduction of the problem. Chapter 2 summarizes developments of RF communication to show how technological changes affected the communication technology. In Chapter 3, underwater communication

types, methodologies used and the channel capacity for underwater communication are discussed. Then, we summarized the existing technologies. In Chapter 4, we explained the idea behind this thesis and where it is inspired from. In chapter 5, we put forward the design of our 5G Underwater Technology. The next chapters discuss the simulation and test results.

# 2. SUMMARY OF RF COMMUNICATION

## 2.1 1 G to 5G Evolution of Communication Technology

Telecommunication technology has evolved very fast since the last 50 years. Especially in the last 25 years, the increase in the mobile users and the coverage of mobile telephone base station have increased beyond our expectation. The mobile users have now started to exceed the conventional telephone users. A short summary about the evolution of the mobile telephone technology is given in the subsequent paragraphs.

1G (The First Generation) mobile telephone communication technology aimed at satisfying the basic need for voice based communication. Therefore, 1G mobile system provided analog voice communication only. 1G Analog Telecommunication standard was introduced in 1980's and continued until being replaced by the Second Generation Digital Telecommunication infrastructure in late 1990 [12].

2G technology offered short message services (SMS) as an additional service to the 1G voice transmission only services. In addition to that, 2G technology opened the door from analog to digital communication. The 2G technology, shaped in late 1980's, started to be used in late 1990's. The voice transmission was established by digital processing with a speed up to 64 kbps. The bandwidth required for 2G transmission is between 20- 200 kHz. 2G used Time Division Multiple Access (TDMA) and Code Division Multiple Access (CDMA) based standards. During the second generation, mobile telecommunication industry experienced an exponential growth in terms of subscribers and the value added services [12].

The 3G (third generation) technology was developed in 2000. Comparing 3G to previous 1G & 2G technologies, data transmission speed in 3G has been increased up to nearly 2Mbps which is much higher than the speed provided by 2G technologies. The 3G technology was the starting point for the development of smart phones. Moreover, the bandwidth and the speed of mobile communication started to be increased so as to accommodate web-based applications and audio and video files. In addition to those new features, the 3G technology enabled people to download media through the internet due to the increased bandwidth.

The 4G LTE (Long Term Evolution) technologies offers a speed of up to 100 Mbps which is 50 times faster than 3G technology. This new technology has enabled mobile system users to connect throughout at a very high speed. The 4G LTE technology has provided several new technologies such as multimedia, entertainment, and mobile applications, digital television. Although some of the services are also supported by 3G technology, the 4G technology provide larger bandwidth and transmission speed as compared to 3G.

## 2.2 5G RF Communication Technology

The most recent technology for mobile communication is 5G mobile technology which is based on OWA (Open Wireless Architecture) and Open Transport Protocol (OTP). This technology provides almost 1000 times bigger network capacity than existing LTE does.

The 5G Technology is a millimeter wave technology which may face multipath problems due to the high frequency electromagnetic wave propagation in the air. The same problem is also valid for underwater Submarine communication. In this thesis, the multipath problem in submarine communication is investigated in detail.

5G is expected to emerge as a network that will not only connect people to each other, but also connect and control machines, objects and devices. 5G aims at achieving very high transmission speeds of several Gbps, with ultra-low latency. The ultra-lag time is expected to appear for “Internet of Things” rather than individual users. 5G frequency bands are planned and categorized as low band (up to 1 GHz), middle band (1 GHz - 6 GHz) and high band (millimeter wave up to 72 GHz). All of these are currently incompatible and perform very differently from each other. In the future, compatibility issues among them may be eliminated and more harmonious work may be provided.

High frequency bands of 5G technology result in millimeter wave. Therefore, many transmission problems may be faced with a high probability. As the frequency increases, it becomes difficult for the RF waves to propagate through obstacles such as buildings, walls and etc. This propagation problem results in scattering, diffraction and multipath effects as illustrated in Figure 2.1 [25].

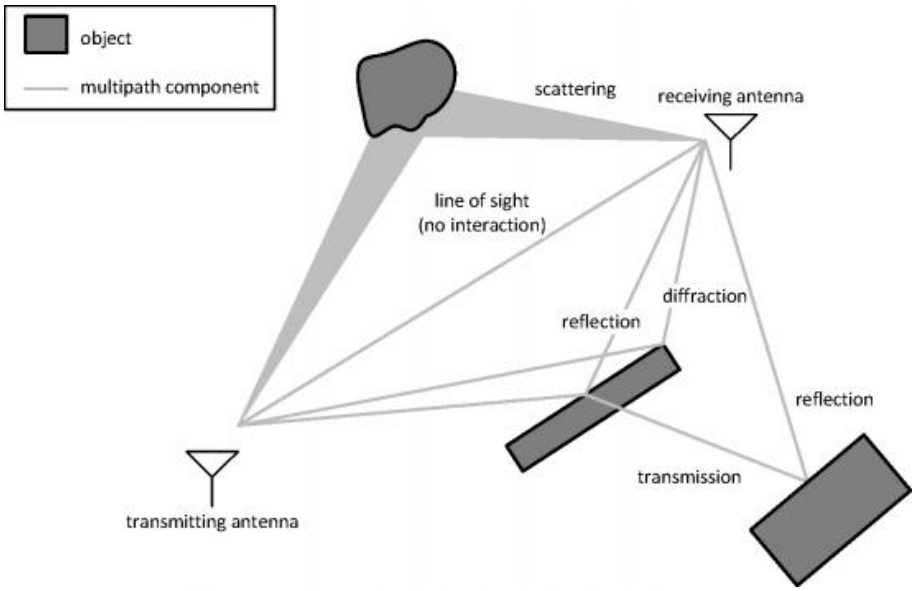


Figure 2.1. Multi Path Effect [25]

5G community has decided to make improvements on both physical (data-link) and transport layers in order to tackle the multipath problem. In the transport layer, MIMO technology and in the data link layer Orthogonal Frequency Division Multiplexing (OFDM) with Polar Codes have been decided to be used by 5G community.

# 3. UNDERWATER COMMUNICATION TECHNOLOGY

As very well known, Sound propagates as a pressure wave under the water. Unfortunately, low frequencies have to be used since sound waves suffer from attenuation. Therefore, acoustic communications are restricted to much lower bandwidths as compared to RF radio communications. Sound speed travels with a maximum speed of 1531 m/s (maximum) at underwater, which in turn limits the available bandwidth for under water acoustic communication. The technology survey indicates that the available commercial and military acoustic modems typically operate within 1 to 100 kHz frequency range. The frequency changes according to applications. In general, underwater voice and data transmission employs frequencies in the 20 kHz - 50 kHz frequency band.

Similar to the design of communications systems, 5G Underwater Acoustic Communication design should consider some design parameters into account. In fact, we have to define our performance criteria before the design. Throughout the history, many known and unknown techniques were used to improve the bit rate of the communication and to increase the range of communication. Although the needs for this communication technology are application specific, the main purpose is to support maximum channel capacity in the maximum distance. In underwater acoustic communication the “maximum” is limited due to the frequency and distance tradeoff. While the frequency increases, the bandwidth also increases. However maximum reachable distance decreases. Although it can be thought that the performance of the acoustic communication can easily be designed by considering the trade between data rate and the communication range, in reality there are several variables that need to be managed. Channel Capacity Approach can be a good performance criterion since it evaluates the system in terms of noise, multipath effect and maximum channel capacity. In this section, the description of performance criteria will be summarized very shortly and further information for attenuation, noise and multipath calculations will be given in chapter 5.

## 3.1 Channel Capacity

As stated before, attenuation, noise, path loss and multipath effects are the main obstacles adversely affecting underwater communication. To overcome these problems, some success criteria should be defined before the design. To calculate the performance of the system, an upper limit is set for the channel capacity based on Shannon-Hartley theorem [14]. Channel capacity is defined by (3.1) stated as

$$C = B \log_2 ( 1 + SNR ) \quad (3.1)$$

C in the Shannon's theorem is the capacity of channel in bps (bits per second), SNR stands for signal to noise ratio and B represents the bandwidth (in Hertz). For the underwater case, if we estimate SNR as 20 dB and the bandwidth of the communication channel as 20 kHz, channel capacity C can be determined as given in Eq. (3.2):

$$C = 20000 \log_2 ( 1 + 20 ) = 87 \text{ kbps} \quad (3.2)$$

This is the upper limit of the channel capacity at 20 dB SNR for a 20 kHz communication channel.

Another point of view for maximum underwater acoustic channel capacity has been put forward in terms of source power and distance between transmitter and receiver. It is stated that maximum data rate is about 100 kbps while the distance is 10 km and the center frequency is 20 kHz [15].

## 3.2 Existing Technologies

The acoustic communication techniques have evolved in line with digital communication technology improvement and developments. New developments of techniques in acoustic communication have allowed acoustic modems to send and receive data over long distances. A detailed literature survey showing the data rates versus distance ranges of some commercially available modems are listed in Table 3.1.

Table 3.1: Acoustic Modem Data Rates & Distance Ranges [13]

| **Product Name** | **Max. Bit Rate (bps)** | **Range (m)** | **Frequency Band (kHz)** |
|---|---|---|---|
| Teledyne Benthos ATM-916-MFI | 15360 | 6000 | 16-21 |
| WHOI Micromodem | 5400 | 3000 | 22.5-27.5 |
| Linkquest UWM 1000 | 7000 | 1200 | 27-45 |
| Evologics S2C R 488/78 | 31200 | 2000 | 48-78 |
| Sercel MATS 3G 34 kHz | 24600 | 5000 | 30-39 |
| L3 Oceania GPM-300 | 1000 | 45000 | Not specified |
| Tritech Micron Data Modem | 40 | 500 | 20-28 |
| FAU Hermes | 87768 | 180 | 262-375 |

Table 3.1 shows that the data rates of acoustic modems available cover a wide range from 40 bps up to 87768 bps. The literature survey indicates that there are mainly three different commonly used frequencies. The first one is 0 – 25 kHz, the other one is 25-50 kHz and the last one is 100 kHz and above. We see that commercially available modems use mainly the frequencies around 25 kHz. This frequency generally supports a good trade between communication range and data rate.

# 4. UNDERWATER 5G TECHNOLOGY PROPOSAL

Underwater communication (UWA) has also improved in line with the improvements in RF Digital Communication. Some variations of the new methods in digital communications are tried to be adapted to UWA communication. However, each improvement necessitates an increase in the communication frequency. Frequency increase in RF communication has a limit and may go beyond the millimeter wave. However, this is not possible for UWA communication due to the limitation imposed by the nature of underwater. High frequency cannot propagate well under the water and it is attenuated very rapidly. Therefore, frequency increase seems not to be applicable for UWA communication.

Although the frequency increase cannot be adapted to UWA communication, some beneficial properties and enhancements of digital communication provides robust UWA communication such as forward error correction methodologies [10] [11]. From the literature research and related works [5], it is observed that the communication problems related to data link layer are very similar to the high frequency RF and UWA communication. Both RF and UWA communication need to cope with multipath and scattering problems. RF 5G technology has already found solutions to tackle with multipath and scattering problems. Using OFDM and a powerful forward error correction method such as Polar Codes are very useful to reduce the multipath and scattering problems.

In this thesis, we propose to use a new transceiver design for UWA communication which offers a robust system against multipath effects while the communication range can be increased due to bit error rate improvements. Our aim is to combine the digital design of data-link layer's control channel of 5G RF Communication with the physical layer of underwater systems. Therefore, data-link layer of RF 5G communication is adapted to underwater communication. Our proposed new design termed as Underwater 5G Technology is also implemented on Xilinx's ZYNQ FPGA. The proposed system consists of two main modules, the first module is the transmitter and the second module is the receiver. Bit error rate and data rate of point to point communication between transmitter and receiver are evaluated as the performance criteria of the proposed system.

# 5. DESIGN AND SIMULATION

The proposed underwater 5G technology system basically consists of a transceiver which includes the hardware and the digital design parts. The Hardware does not provide any additional improvements to existing technologies. However, the Software part includes a proposal about how 5G RF Technology can be adapted to underwater technology.

The digital design of the proposed system consists of three major parts on the transmitter side. The first part is the Input Sampling Part (ISP). ISP accepts data to the system at pre-determined (adjustable from 40 kHz to 100MHz) frequencies. The second part is the symbol creation part which first provides forward error correction encoding and then QPSK modulation is activated for sub-modulation of OFDM. Then, the last stage is the OFDM modulation part. After all of these three operation stages, the signal is ready to transmit.

The Receiver side of the proposed digital design is more complex than the transmitter side. It consists of several subsystems. The first part is the OFDM receiver. Then, the data is extracted and equalized with Zero-Force equalizer. After the equalization, coarse frequency compensation and fine frequency compensation are applied to the received signal. Frequency compensation operations are carried out after the FFT and Equalization processes since there are as much as thousands frequency channels before FFT process and it is very challenging task to apply compensation process to that raw data. Finally, decoding is performed. Each module function is detailed in the subsequent sections. Below, the overall diagram of the system is given in Figure 5.1.

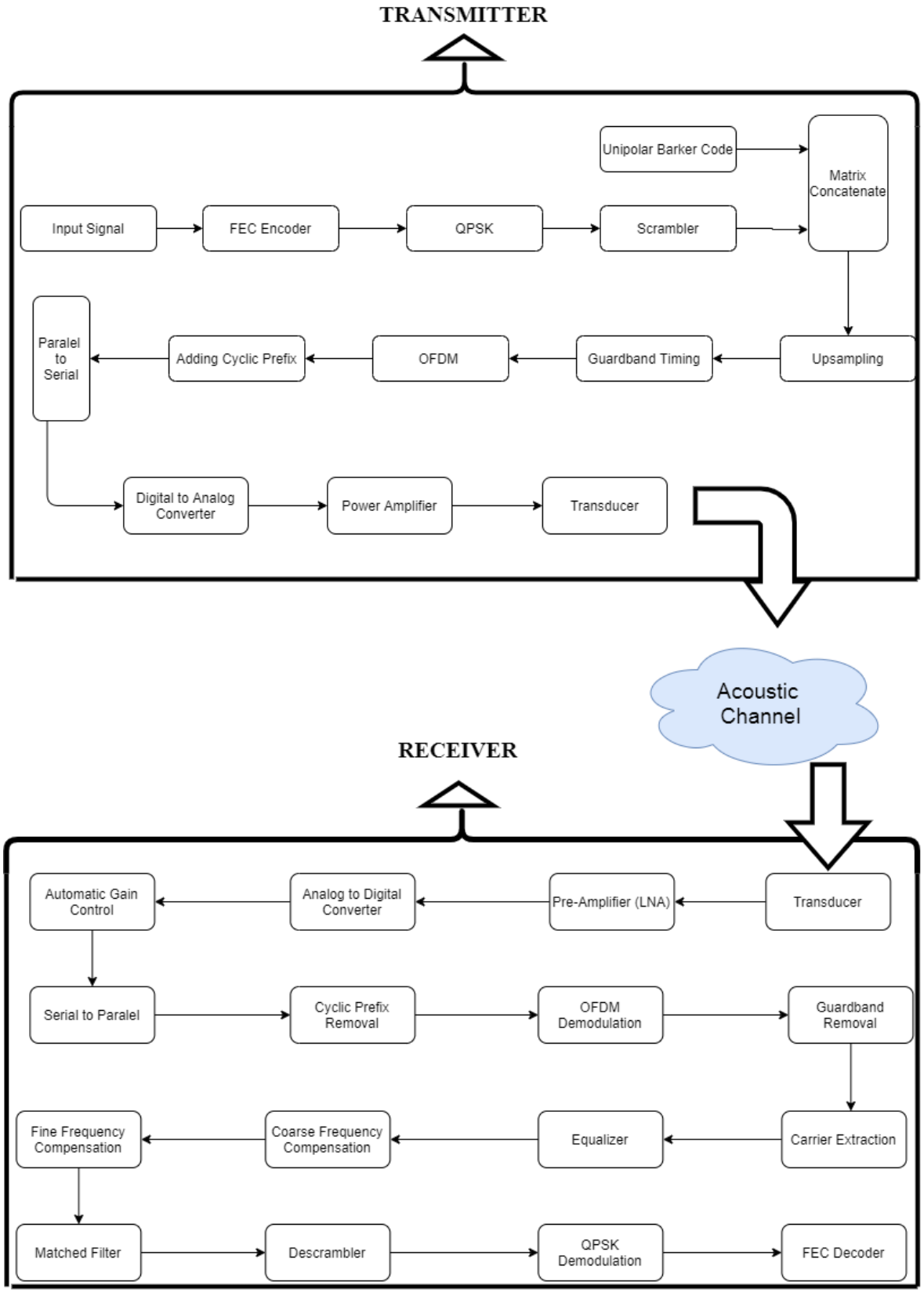


Figure 5.1. The Block Diagram of the Proposed Transmitter and Receiver

## 5.1 Digital Design of the Proposed Transmitter

In this thesis, underwater 5G technology simulations were carried out by using MATLAB software and the system was implemented on Xilinx's FPGA, Therefore, the system is designed by System Generator blocks on MATLAB. The proposed design is suitable for creating a valid Axi-Peripheral IP which can be implemented on any Xilinx's FPGA. The design includes only the basic elements such as logic gates, adders and delay elements. However, sometimes the basic blocks are not enough to implement the desired algorithm. In such cases, Black Box block of System generator is used. When one writes a code block by using VHDL language, the code block with a few modifications can be used as part of MATLAB simulation with the help of "Black Box" block of System Generator. Therefore, in the digital design of our novel system which is called Underwater 5G Technology, only System Generator blocks were used to make the system directly applicable to any Xilinx's FPGA [16].

### 5.1.1 Input Sampling

On the transmitter side, incoming data are sampled with minimum 48 KHz. However, the incoming bits are not directly passed through the transmitter system. They are scrambled via a polynomial before sending the bits to the transmitter. The objective of the scrambling is to decrease the number of consecutive 1s or 0s in the transmitted signal because long sequence of 1s or 0s can cause synchronization problems in the transmission. The scrambler block diagram is shown on Figure 5.2.

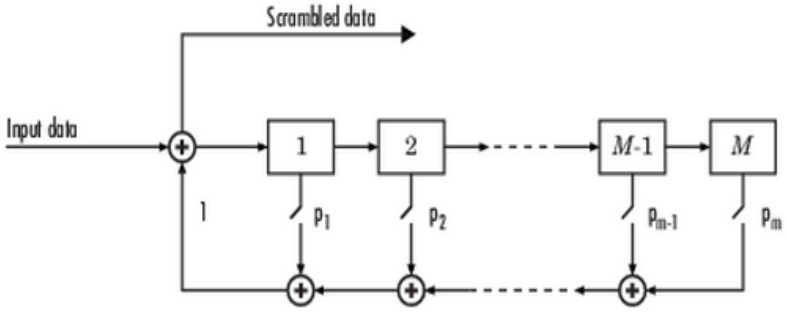


Figure 5.2. Block Diagram of the Scrambler [21]

Each switch of the scrambler is binary so they can be switched on or off and the polynomial of the Scrambler decides whether each switch is on or off. The polynomial

must be chosen as a character vector, such as $1 + z^{-4} + z^{-6}$. In this thesis, the scrambler polynomial is chosen as [1 1 1 0 1] which indicates the power of z. This polynomial is preferred to be used since it is the most general one that is used for noisy channels.

### 5.1.2 Symbol Creation

Symbol Creation part includes two processes; modulating the message signals and generating the "ready to send" symbols. The candidate modulation types are BPSK, QPSK and 4QAM with two-dimensional Gray scale mapping [2] [3].

In this part, not all of these three candidate modulations were implemented to the system. QPSK vs QAM performance analyzes are done in many literature resources [18] in which we can decide that QPSK will give better efficiency in a noisy underwater acoustic multipath channel. For this reason, only the QPSK modulation is implemented with System Generator blocks and will be implemented on FPGA as a part of Underwater 5G System [18]. Performance of the M-ary modulation schemes are shown on Figure 5.3.

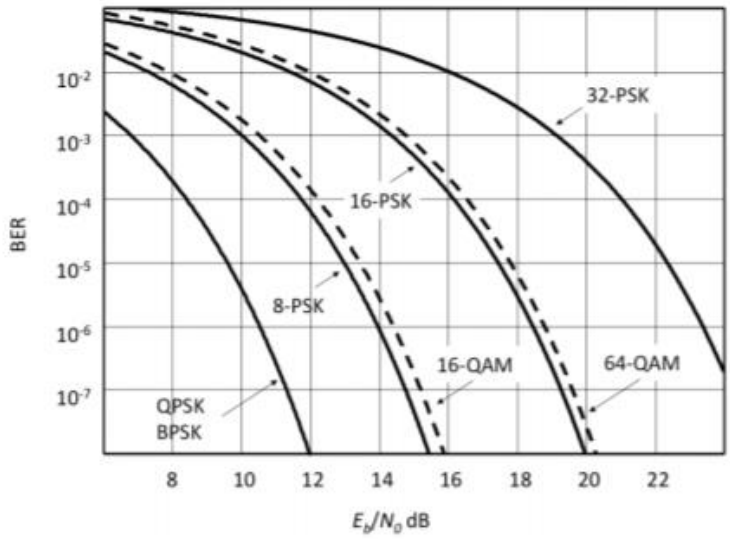


Figure 5.3. BER Perfotmance of M-Ary Digital Modulations [18]

#### 5.1.2.1 Forward Error Correction

Forward Error Correction (FEC) is one of the most important part of Underwater 5G Technology. It decreases Bit error rate significantly. Polar Codes are chosen for Forward Error Correction. The Polar Codes are also chosen for RF 5G Technology. Polar Codes has attracted so much attention recently and it is chosen as the 5G communication standard. The polar codes implementation for 5G by 3GPP community is still going on [19]. However, research on the performance analysis of the Polar Code implementation for UWA communication is mature and there is only one research on this issue [11]. Therefore, it is difficult to comment on the Polar Code performance. In this thesis, Polar Codes are chosen to be used for Underwater 5G Technology to see and contribute to the implementation performance.

"The basic idea of polar coding is to create a coding system where one can access each channel coordinate individually and send data only through those which are the nearest ones." stated in Arikan's paper [20]. Polar encoding design multiplies the matrix of incident message bits with a generator matrix and simply polar codes are generated. After the polar codes are generated, frozen bits are chosen. Polar code generation operation is explained below.

Polar coding block includes 2 parts; first one is the information bits, known as message bits and the other part contains frozen bits. Frozen bits are known bits in both the receiver and the transmitter that help to recover damaged bits. The information bits are multiplied by a generator matrix to create polar symbols.

Mathematical expression of polar code equation can be written as in (5.1). Here, N represents the total number of bits transmitted over the channel, u symbolizes frozen bits and x represents message bits.

$$x_1^N = u_1^N \cdot G_N \tag{5.1}$$

Visualization of a (8, 4) polar code is shown in Figure 5.4. In the notation of (8, 4), the number "8" represents the total number of bits and "4" represents the number of information bits.

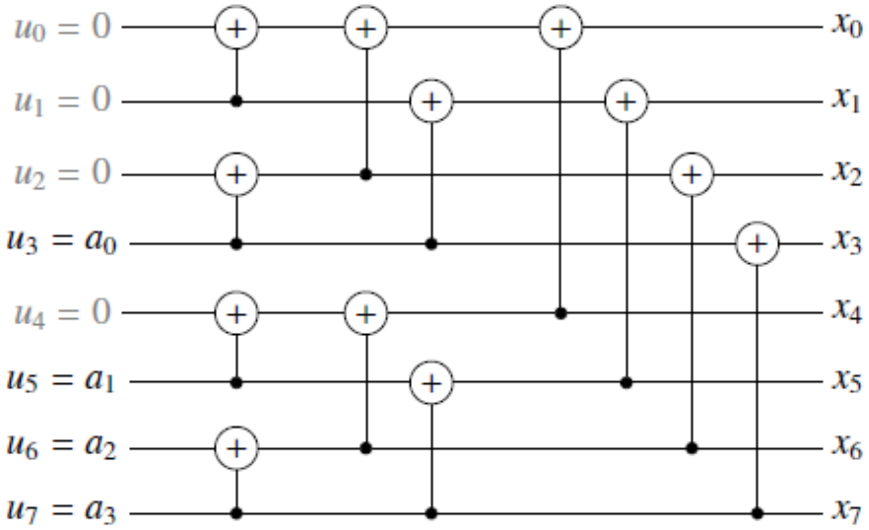


Figure 5.4. Polar Encoding Graph Representation

The "⊕" operator represent the XOR process. For example, to generate $x_0$ message bit related to equation (5.2) is performed.

$$x_0 = [ ( u_0 \oplus u_1 ) \oplus u_2 ] \oplus u_4 \quad (5.2)$$

Other symbols are also calculated in the same way. This process is repeated until each block is encoded.

For the digital design of the FEC, Black Box is used and VHDL code is inserted to the Black Box. A snapshot of the code can be seen in Figure 5.5.

```
CALCULATE_OUTPUT: process(clk)
begin
    if rising_edge(clk) then
        if data_en = '1' and CE = '1' then
            data_out(0) <= a(7) xor a(11) xor a(13) xor a(14) xor a(15) xor a(19) xor a(21) xor a(22) xor a(23) xor a(2
            data_out(1) <= a(7) xor a(11) xor a(13) xor a(15) xor a(19) xor a(21) xor a(23) xor a(25) xor a(27) xor a(2
            data_out(2) <= a(7) xor a(11) xor a(14) xor a(15) xor a(19) xor a(22) xor a(23) xor a(27) xor a(30) xor a(3
            data_out(3) <= a(7) xor a(11) xor a(15) xor a(19) xor a(23) xor a(27) xor a(31) xor a(35) xor a(39) xor a(4
            data_out(4) <= a(7) xor a(13) xor a(14) xor a(15) xor a(21) xor a(22) xor a(23) xor a(29) xor a(30) xor a(3
            data_out(5) <= a(7) xor a(13) xor a(15) xor a(21) xor a(23) xor a(29) xor a(31) xor a(37) xor a(39) xor a(4
            data_out(6) <= a(7) xor a(14) xor a(15) xor a(22) xor a(23) xor a(30) xor a(31) xor a(39) xor a(46) xor a(4
            data_out(7) <= a(7) xor a(15) xor a(23) xor a(31) xor a(39) xor a(47) xor a(55) xor a(63);
            data_out(8) <= a(11) xor a(13) xor a(14) xor a(15) xor a(25) xor a(27) xor a(29) xor a(30) xor a(31) xor a(
            data_out(9) <= a(11) xor a(13) xor a(15) xor a(25) xor a(27) xor a(29) xor a(31) xor a(43) xor a(45) xor a(
            data_out(10) <= a(11) xor a(14) xor a(15) xor a(27) xor a(30) xor a(31) xor a(43) xor a(46) xor a(47) xor a
            data_out(11) <= a(11) xor a(15) xor a(27) xor a(31) xor a(43) xor a(47) xor a(59) xor a(63);
            data_out(12) <= a(13) xor a(14) xor a(15) xor a(29) xor a(30) xor a(31) xor a(45) xor a(46) xor a(47) xor a
            data_out(13) <= a(13) xor a(15) xor a(29) xor a(31) xor a(45) xor a(47) xor a(61) xor a(63);
            data_out(14) <= a(14) xor a(15) xor a(30) xor a(31) xor a(46) xor a(47) xor a(62) xor a(63);
            data_out(15) <= a(15) xor a(31) xor a(47) xor a(63);
            data_out(16) <= a(19) xor a(21) xor a(22) xor a(23) xor a(25) xor a(27) xor a(29) xor a(30) xor a(31) xor a
            data_out(17) <= a(19) xor a(21) xor a(23) xor a(25) xor a(27) xor a(29) xor a(31) xor a(51) xor a(53) xor a
            data_out(18) <= a(19) xor a(22) xor a(23) xor a(27) xor a(30) xor a(31) xor a(51) xor a(54) xor a(55) xor a
            data_out(19) <= a(19) xor a(23) xor a(27) xor a(31) xor a(51) xor a(55) xor a(59) xor a(63);
            data_out(20) <= a(21) xor a(22) xor a(23) xor a(29) xor a(30) xor a(31) xor a(53) xor a(54) xor a(55) xor a
            data_out(21) <= a(21) xor a(23) xor a(29) xor a(31) xor a(53) xor a(55) xor a(61) xor a(63);
            data_out(22) <= a(22) xor a(23) xor a(30) xor a(31) xor a(54) xor a(55) xor a(62) xor a(63);
            data_out(23) <= a(23) xor a(31) xor a(55) xor a(63);
            data_out(24) <= a(25) xor a(27) xor a(29) xor a(30) xor a(31) xor a(57) xor a(58) xor a(59) xor a(60) xor a
            data_out(25) <= a(25) xor a(27) xor a(29) xor a(31) xor a(57) xor a(59) xor a(61) xor a(63);
            data_out(26) <= a(27) xor a(30) xor a(31) xor a(58) xor a(59) xor a(62) xor a(63);
            data_out(27) <= a(27) xor a(31) xor a(59) xor a(63);
            data_out(28) <= a(29) xor a(30) xor a(31) xor a(60) xor a(61) xor a(62) xor a(63);
            data_out(29) <= a(29) xor a(31) xor a(61) xor a(63);
```

Figure 5.5 VHDL Code of Polar Encoder

### 5.1.2.2 Quadrature Phase Shift Keying (QPSK)

QPSK is an M-Ary Phase Shift Keying (M=4) modulation scheme where each symbol is represented by two bits. Normally, the phase carriers are represented by one of these four equally spaced values which are 0, $\pi/2$, $\pi$ and $3\pi/2$. These are the symbols that each one corresponds to a pair of transmitted message bits. Each phase change represents a pair of the digital data. The signal basis for QPSK can be defined as:

$$s_i(t) = \left\{ \sqrt{\frac{2E}{T}} \cos\left(2\pi f_c t + (i-1)\frac{\pi}{2}\right), \quad 0 \le t \le T \right. \tag{5.3}$$

Here, i=1,2,3,4 and $f_c = n_c \frac{1}{T}$, and $n_c$ is an integer number.

Where, T is the duration of the symbol which is two times of the bit period. E represents the energy of the symbol and $f_c$ is the carrier frequency. Constellation diagram of the QPSK is shown in Figure 5.6.

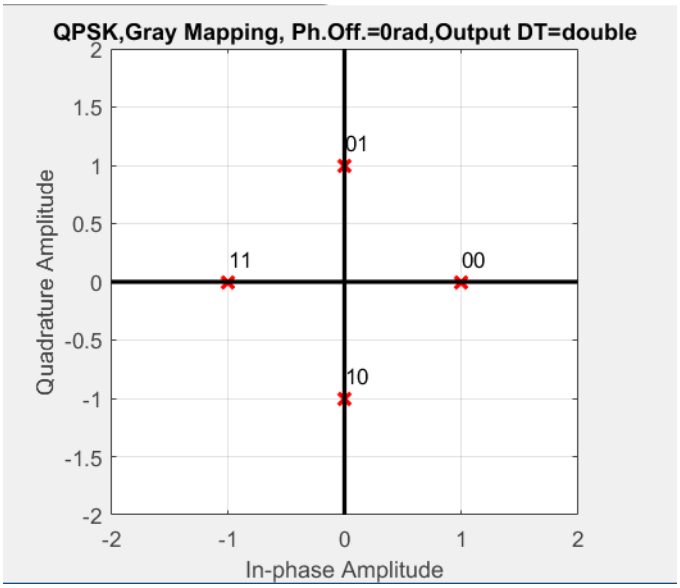


Figure 5.6 : Constellation Diagram of QPSK

As each symbol is represented with two bits, there can be phase jumps in the transmitted signal as much as 180° for two consecutive data. On the transmitter side, when a filter is applied to the signal, large amount of fluctuations can occur due to the mentioned phase-shift. If we offset the timing of the odd and even bits by a fixed symbol period time such as 1 or 0.5, we can prevent in-phase and quadrature components from change at the same time. Therefore, phase-shift can be restricted to the maximum value of 90° at a time if we use this methodology. This results in a more stable signal for the OFDM modulation. This type of QPSK is called Offset-QPSK (OQPSK).

In this thesis, OQPSK is decided to be the modulation scheme for underwater 5G Technology, since it decreases amplitude fluctuations and establishes more stable signals for OFDM modulation. More stable signal means less envelop fluctuations which reduces peak to average power ratio (PAPR). However, our main purpose is not reducing PAPR to zero since we will not use our non-linear element which is Power amplifier in high gain mode. In the OQPSK, the offset can be chosen as, $\pi/4$, $\pi$, $3\pi/4$ and etc. $3\pi/4$ offset is chosen for OQPSK in our design for underwater 5G system. Comparison of symbol transitions between QPSK and OQPSK Constellation diagrams is given in Figure 5.7.

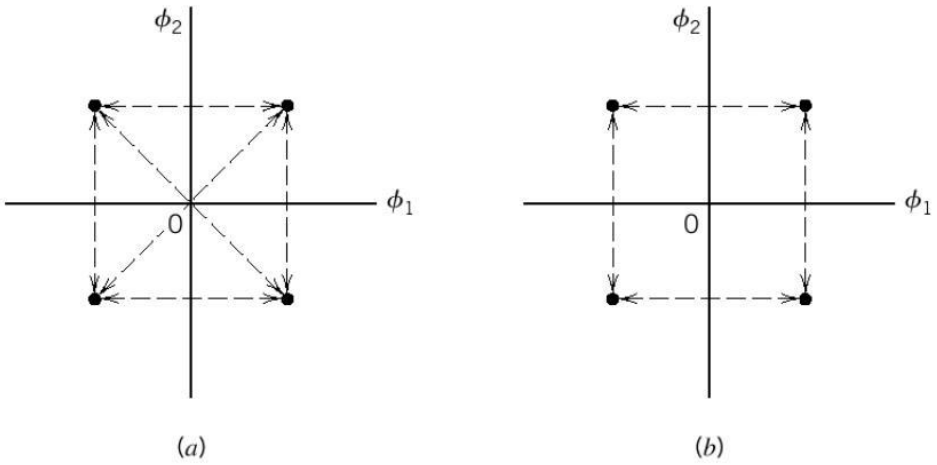


Figure 5.7 : Possible symbol transitions of a) QPSK and b) OQPSK

In this thesis, the proposed digital design of the 3π/4 OQPSK is shown in Figure 5.8:

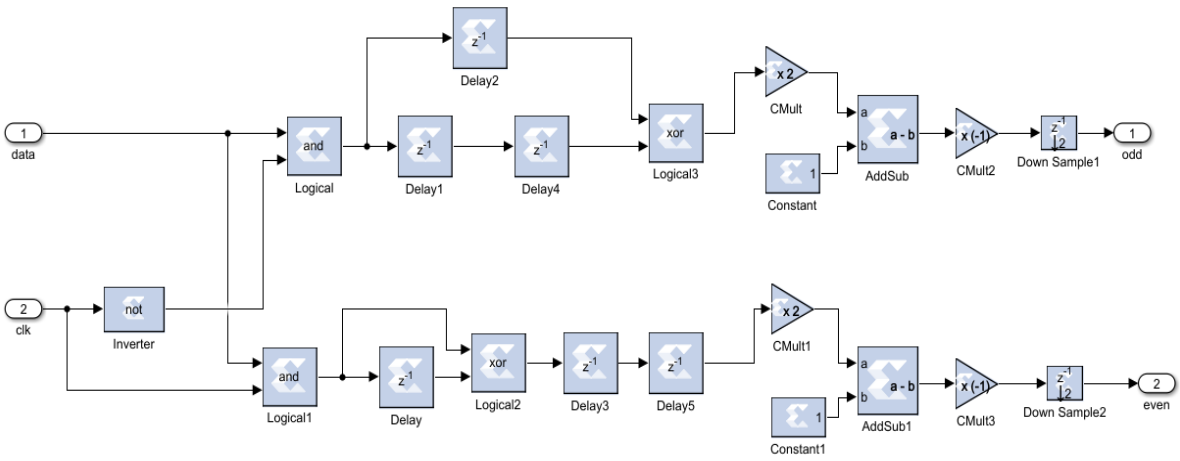


Figure 5.8 : QPSK Modulation

In this design, odd and even outputs represent the In-phase and Quadrature components. As shown in Figure 5.8, QPSK modulation has been evolved to 3π/4 OQPSK by giving the offset time to the even bits. The proposed design above modulates the incoming data by 3π/4 OQPSK. To verify the design, we modulate the same data with the given system and MATLAB's default QPSK block. The proof of the proposed design validation is shown in Figure 5.9. The proposed design and the MATLAB results are compared in Figure 5.10. The results show that the proposed design work the same as MATLAB's block. The only difference is our proposed design is ready to be implemented on FPGA since it is prepared by System Generator blocks.

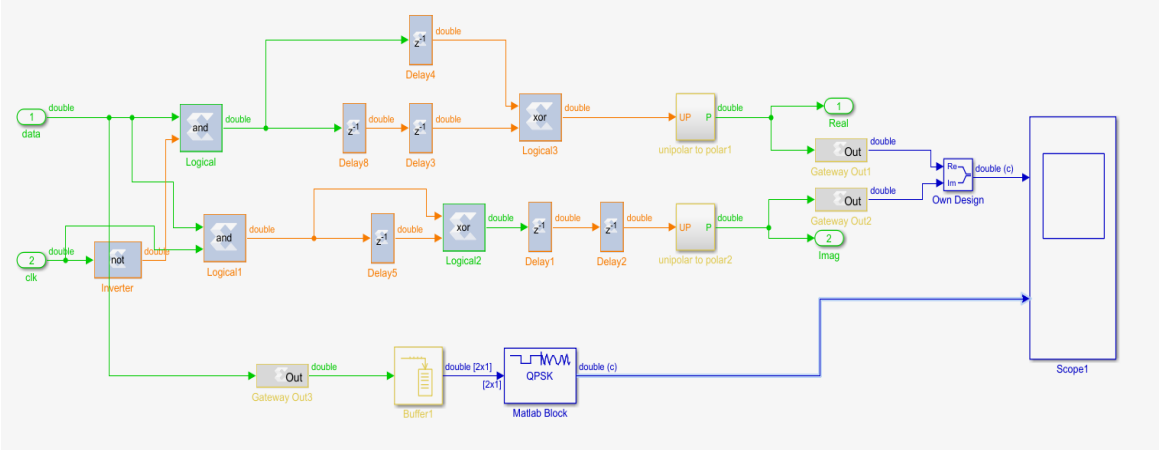


Figure 5.9 : Proof of The System

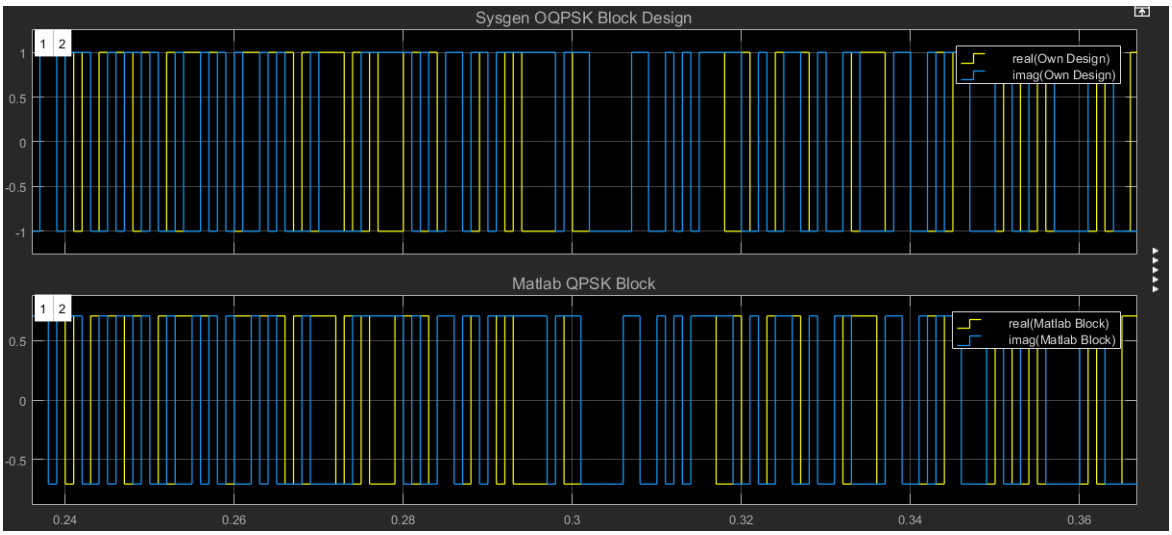


Figure 5.10 : Results of MATLAB block & Own Design

### 5.1.2.3 Barker Codes

To receive a signal especially from a noisy channel, the receiver must know that the incoming signal is not a noise and the signal is worth to be decoded. For this purpose, Barker codes are used in the early generation of RF communication with low data rates such as 1-2 Mbps in the 802.11 standard. Today's RF technology doesn't prefer to use Barker codes. However, Barker may be useful since UWA works on slow data rates such as 0-100 kbps. Therefore, we decided to use barker codes at the receiver side in this thesis. Autocorrelation function or a match filter can detect barker codes at the receiver side where the beginning of the frame can be detected. After the incoming data is scrambled

according to a predetermined polynomial, Barker codes are added at the start of all frames as a preamble. The length of the frames is selected as 384 bits. The details will be discussed on the OFDM transmitter subsection. Each frame includes 384 bits and 26-bit barker code as a preamble is added onto each frame. A match filter checks all the incoming data on the receiver side and if the barker code length is bigger than a threshold value, the frame will be accepted as a valid frame. The use of scrambler and Barker codes are shown in Figure 5.11.

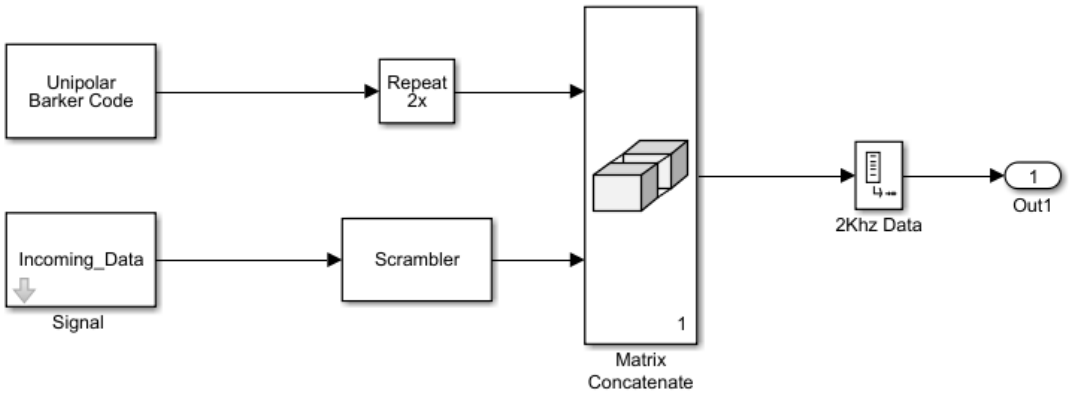


Figure 5.11: Input sampling, Barker codes and Scrambler

### 5.1.3 Orthogonal Frequency Division Multiplexing (OFDM) Transmitter

Orthogonal Frequency Division Multiplexing is a Fourier Transform based multicarrier modulation scheme. OFDM has recently started to be used widely in broad-band wireless communication. It is a multicarrier system where all the symbols are delivered through different sub-channels. Sub-channels are orthogonal to each other. This design enables high data rates and preserves symbol durations being longer than the channel dispersion time. Therefore, OFDM systems can reach high transmission rates safely in time-dispersive or frequency-selective channels. Moreover, channel equalization is not necessary for the RF communication time-domain with this design.

OFDM as a multi-carrier system divides the spectrum into many sub channels with narrow bands. The data is sliced into parallel streams which are carried by different channels as depicted in Figure 5.12

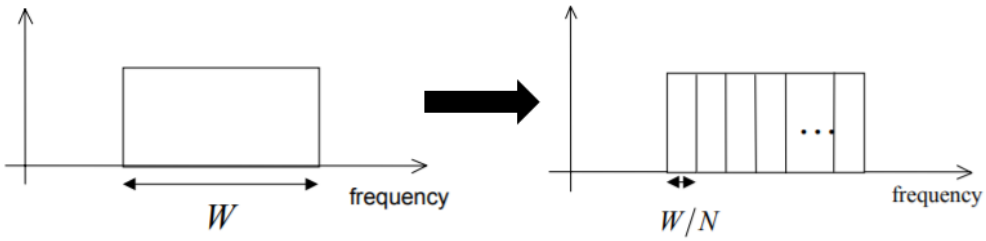


Figure 5.12: OFDM

As shown in Figure 5.12, sub-channels are transferred consecutively. Unfortunately, this situation may cause inter symbol interference (ISI) problem. To overcome this ISI problem, Cyclic Prefix (CP) code is used. That is to state that some amount of data is added at the end of the sub-channel to ensure reduction of ISI. Although CP causes spectral inefficiency, it certainly decreases the bit error rate.

OFDM uses a sub-modulation schema to create symbols that will be transferred via sub-channels. Modulation type used in OFDM changes according to system requirements. In general, BPSK, QPSK and QAM are used as the modulation types.

OFDM has recently been used for underwater acoustic communication due to its robust characteristics for channels that require long propagation delay. Cyclic Prefix and Guard Time features of OFDM facilitates robust communication and provides immunity to inter symbol interferences. The determination and design of cyclic prefix is discussed in the following sections. Here, we can confidently state that it is possible to establish a good and robust underwater communication link by a properly selected Cyclic Prefix.

OFDM is chosen to support broadband communication for high speed RF transmission. However, the situation for underwater is different. Underwater communication cannot support high speed transmission due the nature of propagation under the water where the maximum speed of sound waves is about 1500 m/s. Since OFDM divides the spectrum into many sub channels with overlapping narrow subbands, symbol duration becomes relatively long compared to the multipath spread of the underwater acoustic channel. As a result, Inter Symbol Interference might be neglected in each subband which simplifies the receiver complexity on the receiver side significantly.

This phenomenon motivates researchers to work on OFDM in UWA channels. Therefore, OFDM is a suitable candidate for underwater acoustic communication.

For the 5G Underwater Technology, OFDM transmitter and the Forward error correction are the most important parts since they are directly adapted from RF 5G technology. OFDM transmitter scramble the data first and the symbols are created by using FEC encoder and QPSK modulator. Here, it is necessary to create OFDM symbols. In the subsequent paragraphs, the digital design and the mathematical expression for the UWA OFDM Transmitter is detailed.

#### 5.1.3.1 OFDM Transmitter Mathematical Expressions

OFDM transmitter is chosen for underwater 5G technology since it is one of the most efficient modulation scheme for the noisy multipath channels. To prove mathematically that OFDM symbols can survive in the multipath channel, assume that the channel output $y_n$ can be written as given in (5.4):

$$y[n] = h[n] \otimes x[n] + n[n] \tag{5.4}$$

where $\otimes$ operator denotes the circular convolution, $h_n$ is the multipath tap, $x_n$ is the transmitted message, and $n_n$ is the noise. Mathematical expression of the transmitted message is given in (5.5). Here, "n" denotes the time and "k" symbolizes the modulation index, N represents the up-sampling factor and $a_k$ denotes the modulation symbols which is non-zero in the interval of $0 \leq k \leq N - 1$.

$$x[n] = \sum_{k=0}^{N-1} a_k[n] \cdot e^{j\frac{2\pi}{N}k}, \qquad n = 0, 1, 2, ....., N-1 \tag{5.5}$$

At this point a cyclic prefix (CP) is used to prevent inter block interface and create a circulant channel matrix with length larger than or equal to the maximum channel length (L) [28]. The transmitted signal with CP is a sequence of messages that first N bits of the original transmitted sequence is added at the end or beginning of sequence: $[\mathbf{x}_{N-(L-1)}, \ldots, \mathbf{x}_{N-1}, \mathbf{x}_0, \mathbf{x}_1, \ldots, \mathbf{x}_{N-1}]$. The transmitted message can be written in matrix form by (5.6).

$$\underline{x} = \begin{bmatrix} x[0] \\ ... \\ x[N-1] \end{bmatrix} = Q \cdot \underline{a}$$

(5.6)

where Q represents the DFT matrix for a vector sequence $\{Xn\}_{n=0}^{N-1}$

When the DFT operation is applied to the channel output of $\{y_n\}_{n=0}^{N-1}$ in (5.4)

$$y[n] = \sum_{l=0}^{L-1} h_l(n - l)_N \quad (5.7)$$

Here, $h_l$ denotes the multipath channel, and "l" is the tap number for the multipath channel.

That is to state that each message passing through the channel is affected by 3 multipath. So, we can rewrite "y" in terms of the transmitted signal and channel coefficients as in (5.8).

$$\underline{y} = \underline{H} \cdot \underline{X}$$

(5.8)

H is the convolution matrix and consists of multipath taps in the time domain. H is a circular matrix. Also, open-form of the matrices are given in [28] (5.9).

$$\underline{y} = \begin{bmatrix} h_0 & 0 & \dots & h_2 & h_1 \\ h_1 & h_0 & 0 & \dots & h_2 \\ h_2 & h_1 & h_0 & 0 & \dots \\ \dots & \dots & \dots & \dots & \dots \\ 0 & \dots & h_2 & h_1 & h_0 \end{bmatrix} \cdot \begin{bmatrix} x_0 \\ x_1 \\ x_2 \\ \dots \\ x_{N-1} \end{bmatrix} \quad (5.9)$$

The eigenvalues of H:

$$\lambda_i = \sum_{n=0}^{N-1} h_n \cdot e^{-j\frac{2\pi}{N}n_i}$$

(5.10)

where i = 0, 1, …, N-1

The term $h_n$ is the impulse response of the given multipath channel. Multipath channel can be formulated by the expression given in (5.11).

$$y_n = Q \cdot \Lambda \cdot Q^H$$

(5.11)

where $\Lambda = \text{diag}\{\lambda_k\}$

Considering (5.9), (5.10) and (5.11), the eigenvalues can be proved to be equal to the expression in (5.12).

$$\lambda_k = \text{DFT}[h_0\ h_1\ h_2\ \ ...\ h_{T-1}]$$

(5.12)

To define "y" in terms of "λ", y can be represented as:

$$y_{f,k} = \text{DFT}\{\, y_n \,\} \qquad (5.13)$$

Finally,

$$y_{f,k} = \lambda_k \cdot a_k + n_k\ , \qquad k = 0, 1, 2, \ldots, N\text{-}1$$

(5.14)

The Equation (5.14) indicates that the output of the multipath channel is a product of the multiplication of modulation symbols by the eigenvalues of the multipath channel plus the ambient noise. Now, we can conclude that we can easily recover the incoming data from the multipath effects if we can estimate the channel, To perform this recovery task, we need to design an equalizer with a dynamic given by (5.15).

$$a_k = \frac{1}{\lambda_k} \cdot y_{f,k}\ , \qquad k = 0, 1, 2, \ldots, N\text{-}1$$

(5.15)

This equation is the basis function of the proposed underwater 5G technology and is called Zero-Force Equalizer. At the receiver side, we demonstrated that the bit error rate is reduced significantly when we implemented our equalizer design. Therefore, we can conclude that a stable connection cannot be established between the transmitter and the receiver without using this equalizer. Moreover, Plot insertion is also done in the digital design of OFDM Transmitter for the Equalizer to work properly.

Unfortunately, Zero-Force Equalizer is not sufficient for a proper communication without adding the cyclic prefix to the message signal as shown in (5.7). The length of the Cyclic Prefix (CP) is also crucial for the underwater 5G technology. For the RF communication length of the CP is generally one fourth of the message length. In our thesis, we propose the CP to be chosen as given in (5.16) and (5.17) below [28]:

$$L = [W \cdot \tau]$$
(5.16)

$$\text{Length}(CP) \geq L$$
(5.17)

Our proposal for the CP length is based on the simulation results of our proposed underwater 5G technology.

Where W equals to the total operational bandwidth and $\tau$ is the delay spread in seconds.

#### 5.1.3.2 Digital Design of the Proposed OFDM Transmitter

The first stage in the design of OFDM transmitter is the creation of symbols with QPSK modulation and Forward Error Correction. The second stage is the up-sampling application by a factor of 1/12. This process is called IFFT input packing. The data for which IFFT is performed is packed before the up-sampling process. The details of up-sampling process are shown in Figure 5.13. Here, pre-defined up sampling model is not used. Rather, for every 12 bits pair of data, 12 bits of complex signal is inserted to the system.

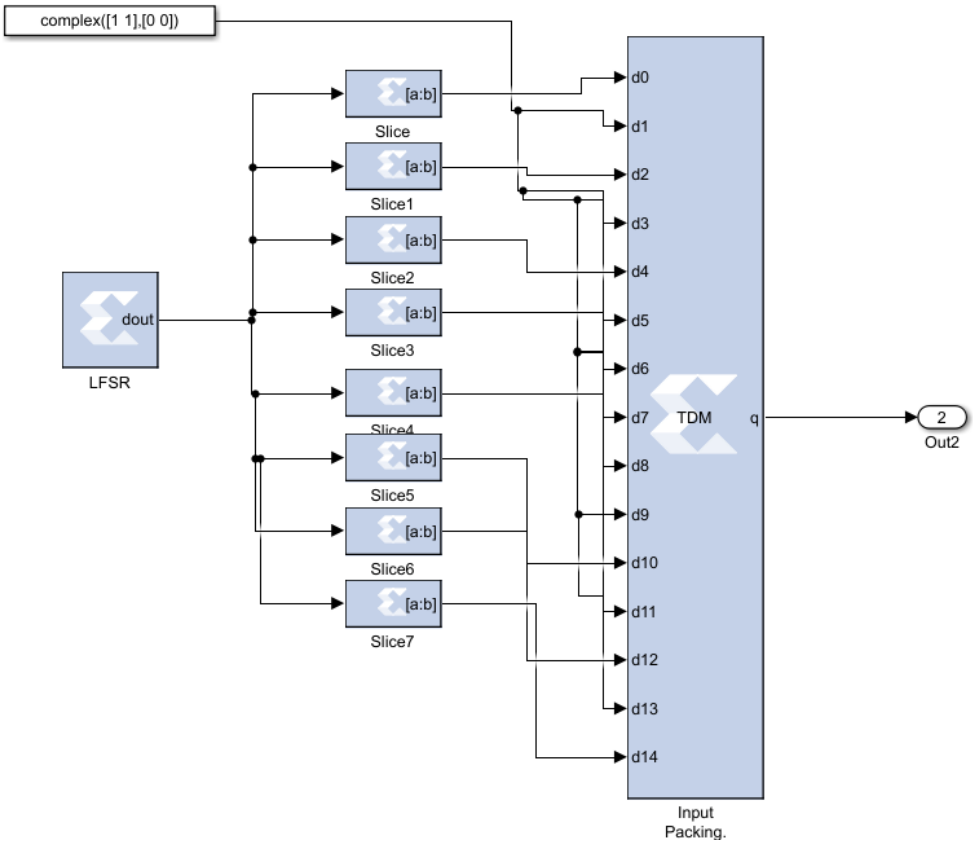


Figure 5.13: Upsampling process

This OFDM structure is termed as the Inverse Finite Fourier Transform (IFFT) process. IFFT of the baseband symbols creates OFDM symbols. In the previous process, input is packed for the OFDM and it becomes ready for the IFFT. However, there is one more additional step for the OFDM which is the addition of guard bands to the message signal. This additional step is crucial for underwater 5G technology. As shown in 5.14, guard bands prevent the Inter Channel Interference (ICI). For the underwater 5G technology, we chose lengths of the guard bands to be 20 ms. We chose this 20 ms with the help monte-carlo simulation methodology. We simulated our system with guard bands and reached least ICI with 20 ms.

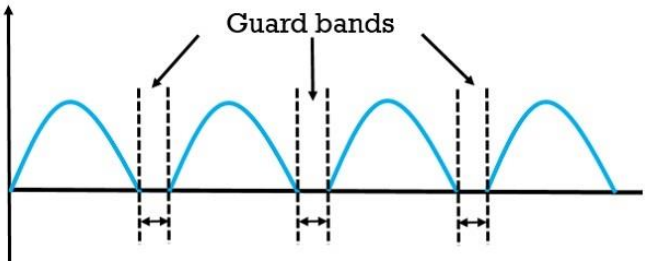


Figure 5.14: Guard bands

After the guard bands are created as they are shown in Figure 5.14. Then, IFFT of the message signal is performed. Finally, CP is added to the end of the transmitted signal. The whole process is shown in Figure 5.15.

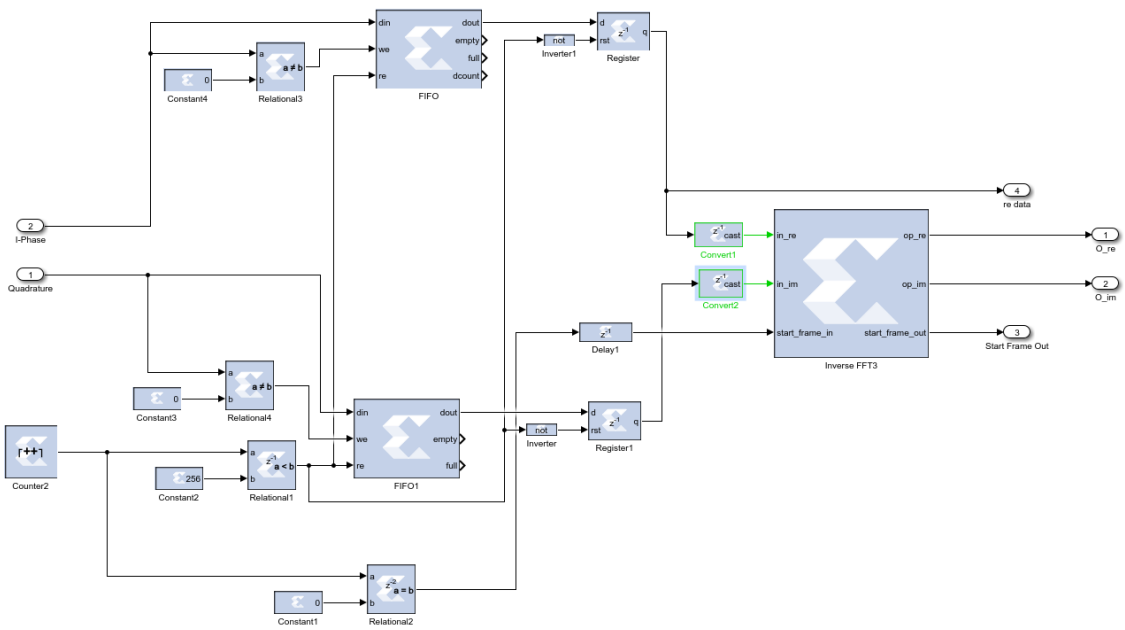


Figure 5.15: IFFT process

In the System Generator Block, we can directly add Black Box and prepare embedded VHDL code for Black Box to perform the specific task. For the guard band generation, a VHDL code block is prepared and it is inserted into the Black Box. VHDL code block is not enough alone. It is also necessary to write a MATLAB code for the Black Box to make it work as desired. Written MATLAB and VHDL codes are given as an Appendix A to this thesis and the Black Box design is depicted in Figure 5.16.

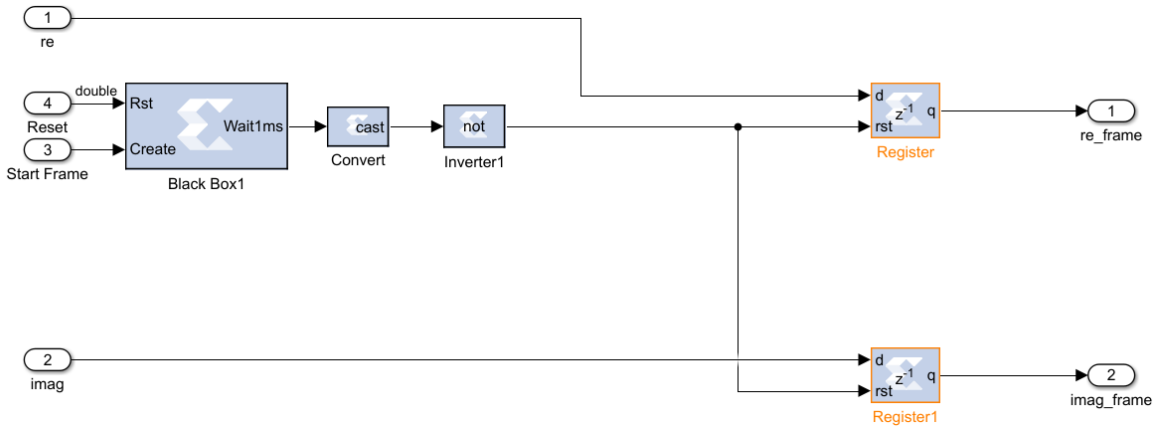


Figure 5.16: Guard band implementation

Ideal length of the CP is given in the Equation 5.7 and it can be calculated for the candidate systems. The flexibility is one of the most important features of the underwater 5G technology. Therefore, the parameters can easily be adjusted for different data rates For example, in a channel that has 10 millisecond delay spread and 5 kHz operational bandwidth, the CP length should be minimum 50. Below, our proposed design with CP addition is shown in Figure 5.17.

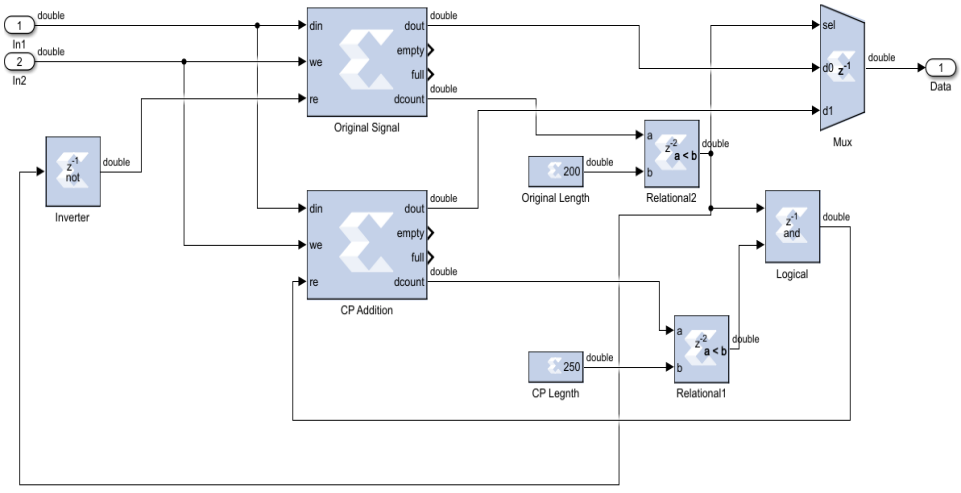


Figure 5.17: Cyclic prefix addition

Final part of the OFDM transmitter is the transition to the pass band. This process carries base band signal to pass band. There are several options for this process. Base Band to Pass Band process is chosen to implement for the underwater 5G technology.

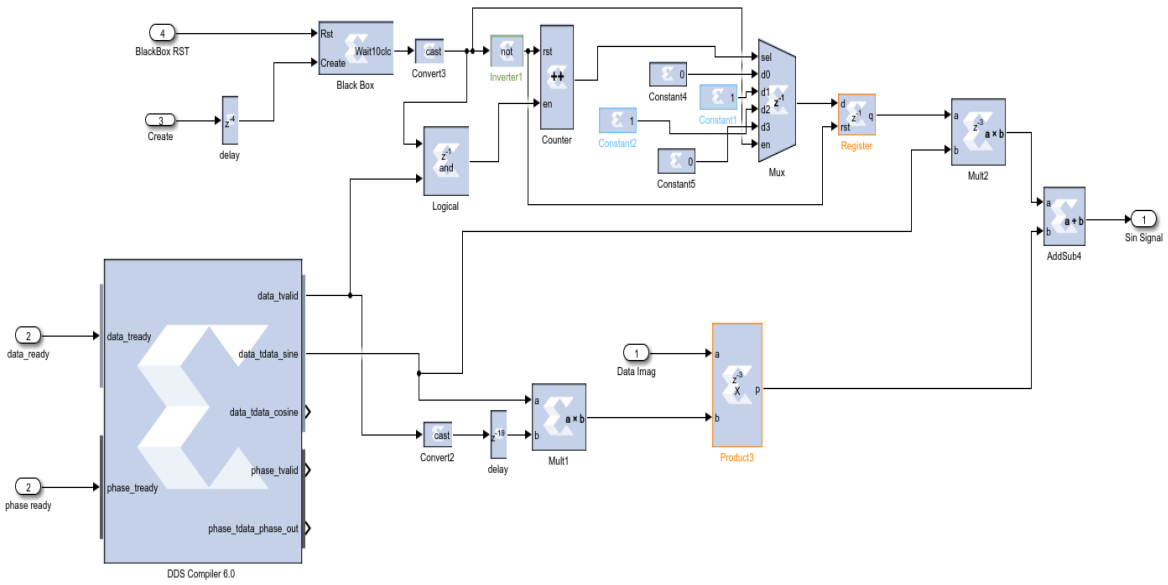


Figure 5.18: Baseband to Pass Band

## 5.2 Digital Design of the Proposed Receiver

Digital design of the receiver requires more effort compared to transmitter since it is harder to sense a noisy acoustic signal then creating it. Therefore, receiving process consists of many sub modules. Firstly, the incoming signal transduced to a based band signal via a proper low pass filter and main noises are eliminated from the signal. Then, by the help of the acoustic channel estimation, the signal is equalized and what remains only is its necessary data part. Finally, the signal is decoded. Details of the process are explained below.

### 5.2.1 Digital Design of OFDM Receiver

The main objective of the receiver is to have the incoming data with minimum noise as minimum as possible. There are two main modules which play crucial roles in the design of the receiver. The first module is a well-designed low pass filter to remove the ambient noise. In this thesis, the low pass filter is designed by using the FDA (Filter Designer and Analyzer) module of the System Generator. Once the ideal low pass filter is designed, FDA determines the filter coefficients which are easily adapted to the filter. Designing a robust filter is not trivial since there are many tradeoffs such as the order of the filter and its superior free dynamic range. After trying several implementations, a low pass filter with an excellent performance for underwater 5G technology is designed and implemented. The order of the filter is 201. The order of the filter is relatively high, it is

chosen in that way to increase spurious free dynamic range and since we used ZYNQ FPGA, this order of filter doesn't cause any memory related problems. The Magnitude and the Phase response of the filter is shown in Figure 5.19 and Figure 5.20.

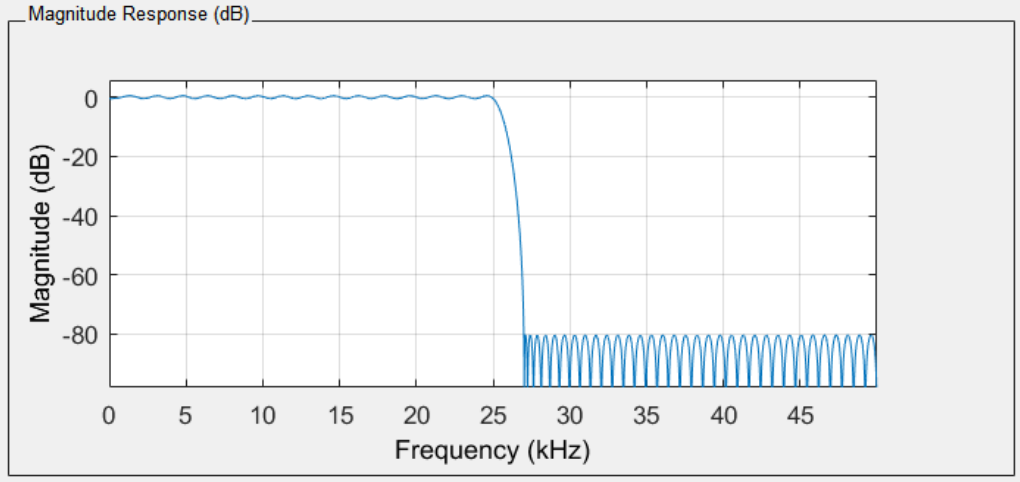


Figure 5.19: Magnitude response of the Low-pass filter

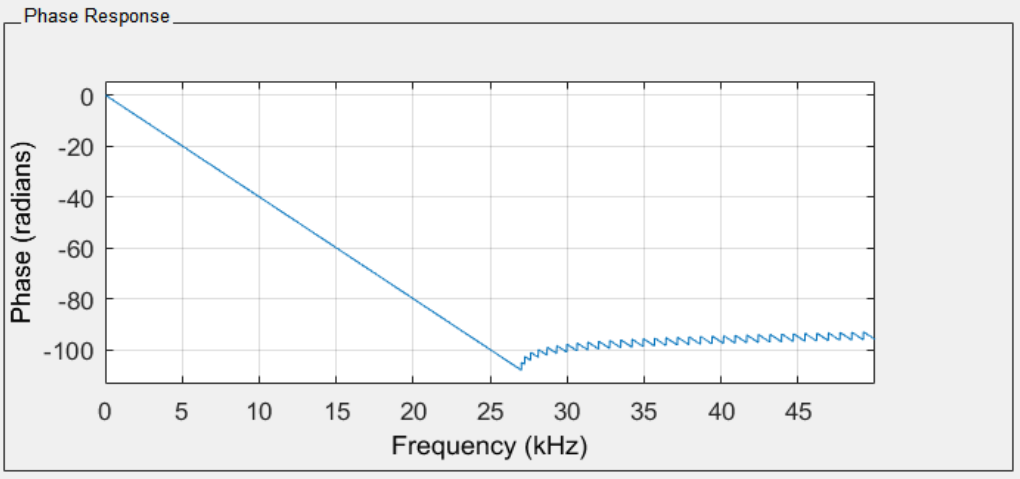


Figure 5.20: Phase response of the Low-pass filter

The filter is designed for the transmitted signal whose carrier frequency is 25 kHz. As shown on figure 5.19, the magnitudes of the signals above 25 kHz are eliminated precisely. Second important graph for the filter is the Phase response graph. If the frequency doesn't change linearly with the phase response in the active area of the filter, signal decays. However, in our filter design, it is clearly shown on Figure 5.20 that

frequency linearly changes with the phase of the signal. This property is a desired property for non-distorted communication.

The second module is the gain control and the normalization operations module. To treat each data equally, they have to be normalized. In addition, the signal level should be controlled by a gain controller. Then, Cyclic Prefixes must be detached from the incoming signal. The digital design of this gain control and normalization of OFDM receiver for underwater 5G technology is shown in Figure 5.21.

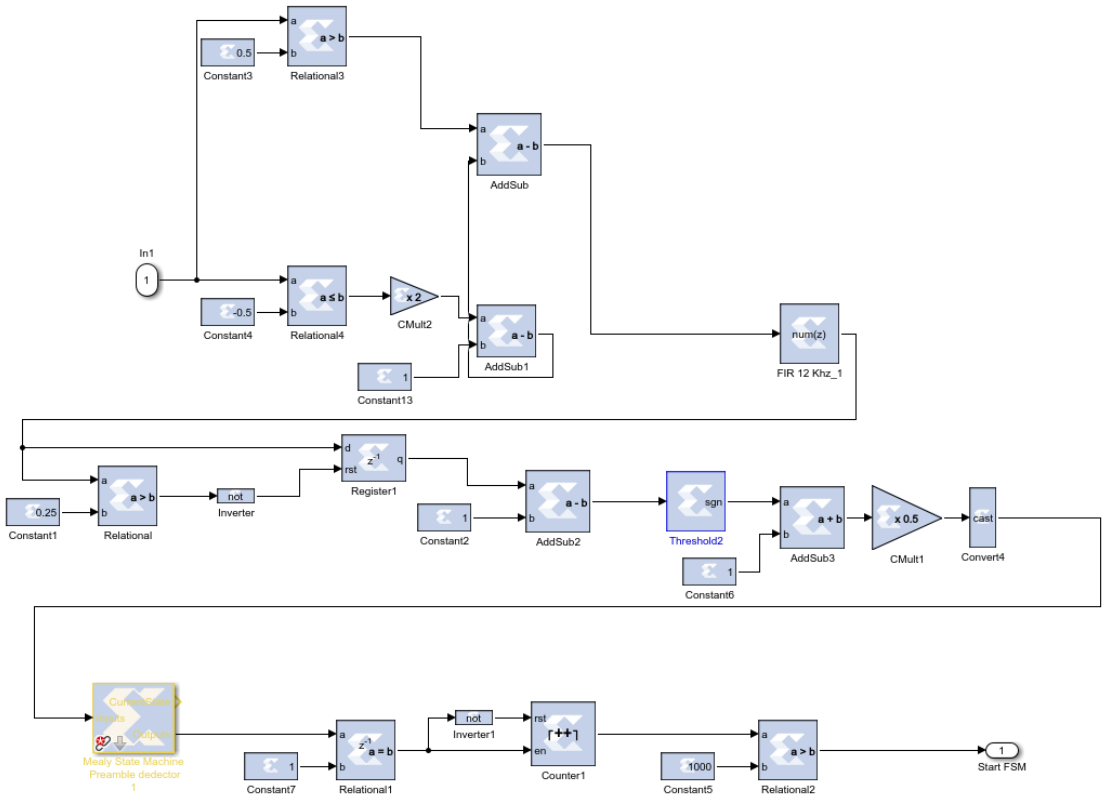


Figure 5.21: Gain control and normalization

Once the signals are normalized and filtered, the next thing is to convert OFDM symbols to the QPSK symbols. Each OFDM symbol is carried via a different channel, to create these channels, we used IFFT on the transmitter side to create a frequency bin from these multiple channel streams. On the receiver side, the carriers must be extracted and mentioned frequency bins must be divided into different streams again. For this purpose, we applied FFT to the incoming signal. FFT process extracts the symbols. However there are residual guard bands which were added on the transmitter side. Location of the guard

bands are saved in a memory unit which is a trivial task. Digital Design of the FFT process is shown on Figure 5.22.

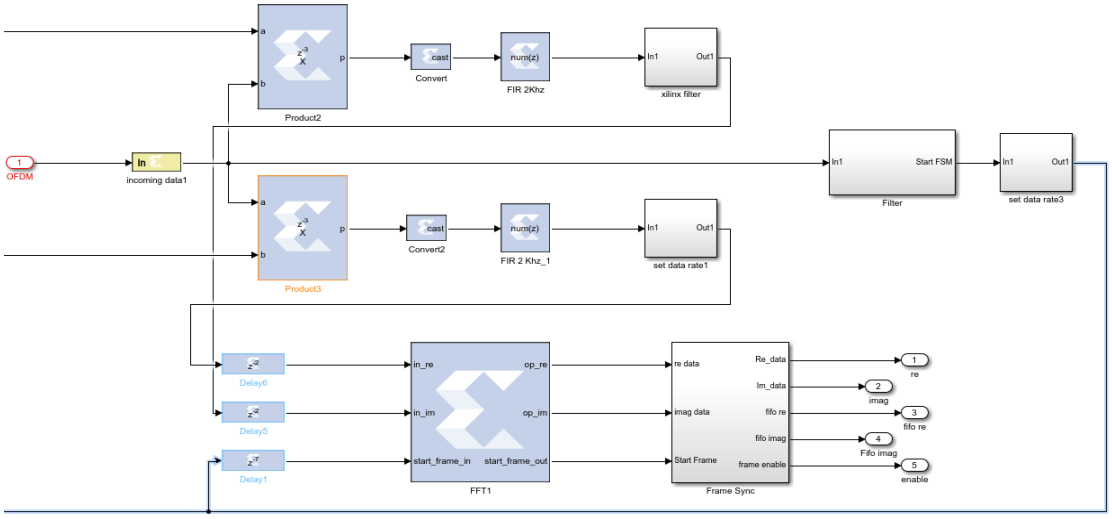


Figure 5.22: FFT Process

Taking FFT with the System Generator block is not same as a normal FFT process, the system must know the right time for the start of the FFT process. Otherwise, the FFT doesn't give the desired symbols. For this purpose, a Frame Synchronization Block is designed. This design helps to detect the valid frame for the remaining part of the receiver. Digital design of the frame synchronization is shown in Figure 5.23.

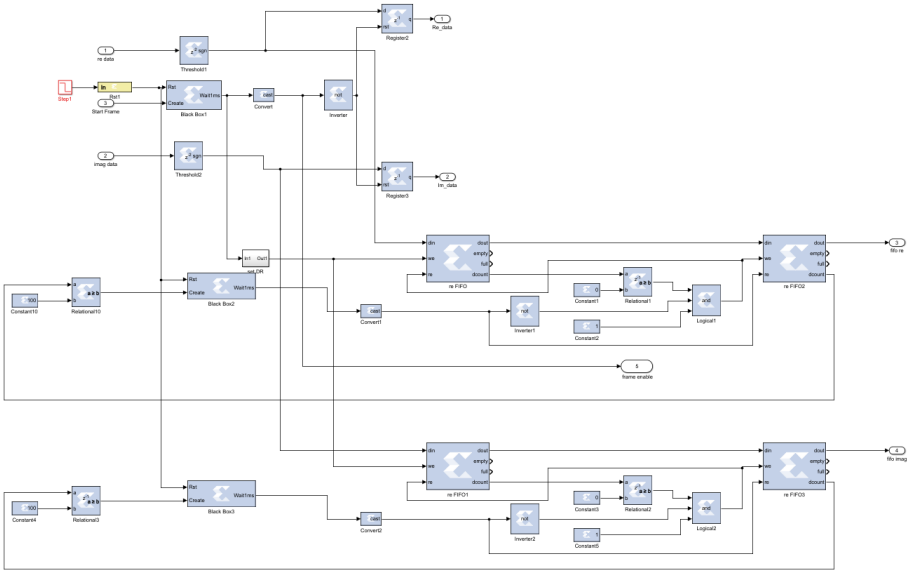

Figure 5.23: Frame synchronization

### 5.2.2 Acoustic Channel Estimation

Our proposed design for underwater 5G technology system aims at offering a robust system for the noisy channels. For this purpose, acoustic channel estimation is included in the receiver part. This estimation methodology helps to overcome not only multipath components and frequency offsets but also ambient noise, phase offsets and Doppler effects on the message symbols.

First part of the estimation is the channel equalization part. With the help of a proper equalization methodology, baseband QPSK symbols are reconstructed and this process enables the work compensation methodologies. Without proper channel equalization, we cannot apply any compensation or decoding algorithms since the signals are corrupted. After the equalization process, the received signal becomes ready to be corrected in terms of phase and frequency offsets, for this purpose two important blocks are designed. The first one is the Coarse Frequency Compensation which estimates and corrects the phase and frequency offset. The second block is the Fine Frequency Compensation block which corrects residual components of frequency and phase offsets.

Finally, no special digital design is made for the Doppler Effect since the transmitter and receiver is assumed to be settled to fix points. It is eliminated by the low pass filter at the start of the receiver and compensated with the guard band in the message.

#### 5.2.2.1 Channel Equalization

As mentioned in the “Digital Design of the proposed OFDM Transmitter” section, without a proper equalizer the system cannot establish a good communication. This Equalizer is one of the most important part of the underwater 5G technology. As proved earlier, we have to estimate the channel and then we have to equalize it. The received signals can be expressed in terms of channel response and incoming signals as in (5.24):

$$\underline{Y} = \underline{X} \cdot \underline{H} + \underline{V} \tag{5.24}$$

Here, Y represents the incoming symbols through the acoustic channel, X represents the plot symbols matrix, H is the frequency response of the acoustic channel and V is the ambient noise. Open-form of the matrices are given in (5.25).

$$\begin{bmatrix} y_0 \\ y_1 \\ y_2 \\ \dots \\ y_{N-1} \end{bmatrix} = \begin{bmatrix} x_0 & \dots & \dots & x_2 & x_1 \\ x_1 & x_0 & \dots & \dots & x_2 \\ x_2 & x_1 & x_0 & \dots & \dots \\ \dots & \dots & \dots & \dots & \dots \\ 0 & \dots & x_2 & x_1 & x_0 \end{bmatrix} \cdot \begin{bmatrix} h_0 \\ h_1 \\ h_2 \\ \dots \\ h_{N-1} \end{bmatrix} + \begin{bmatrix} V_0 \\ V_1 \\ V_2 \\ \dots \\ V_{N-1} \end{bmatrix} \quad (5.25)$$

There are many channel estimation methods used for the OFDM such as Minimum Mean Square, Linear Mean Square and Least Square. For the Underwater 5G Technology, Least Square method is chosen to be used as the estimation methodology for the equalizer. The Least Square method estimates $\widehat{H}$ to minimize the cost function of the given as:

$$J(\widehat{H_p}) = \left\| Y_p - \widehat{Y_p} \right\| \quad (5.26)$$

Solution of this Least Square channel estimation is given in (5.27):

$$\widehat{H_{Ls}} = (X_p^H X_p)^{-1} . X_p^H Y_p = X_p^{-1} Y_p \quad (5.27)$$

After the Least Square Estimation is applied, the solutions give us the taps of the multipath channel. These solutions are directly used in the equalizer.

For the digital design of the Equalizer, a Black Box is used from the System Generator Toolbox. Inside of this Black Box, VHDL code is generated to make the calculation of Equation (5.15).

#### 5.2.2.2 Coarse Frequency Compensation

After the channel is equalized and QPSK symbols are extracted from OFDM symbols, the following step in the Acoustic Channel Estimation process is the Coarse Frequency Compensation (CFC). As mentioned before, receiving and transmitting units are two separate and identical units spatially since the incident signals which are sent from transmitter are corrupted by the acoustic channel. Therefore, frequency offsets will occur relatively. This offset may consist of frequency offset and phase noise. However as mentioned above this compensation cannot be done before FFT since there are many sub channels. In this part, frequency and phase offsets of the receiving signal are detected and then they are corrected.

There are two known coarse frequency compensation methodologies in the literature which are data-aided and blind compensation. Data-aided compensation methodologies use the preamble knowledge of the signal to correct the coarse frequency. Although this kind of compensation methodology promises a good rate of correction, its performance depends on the length of preamble. With a correctly chosen preamble, this methodology performs well enough. Since we used two sets of 13 bits barker codes as preamble, data-aided compensation is suitable for our design. Therefore, the frequency offset estimation, a correlation based algorithm known as "Luise Algorithm" is implemented. Luise algorithm present an efficient technique for fast carrier frequency offset recovery based on data modulation and/or channel distortion removal from the received signal. Luise algorithm is based on ML estimation theory, and its error performance in the absence of fading is observed to lie very close to the Cramer-Rao lower bound (CRLB) for unbiased estimators. Luise Estimation Algorithm have good performance and it is easy to implement [21]. Therefore, Luise Algorithm is chosen for our proposed Underwater 5G Technology implementation. For the implementation, the following algorithm is used. After the Luise Algorithm determines the offsets, CFC Algorithm corrects the phase and frequency offsets. CFC block estimates the offsets with the formula in (5.18):

$$\text{estimate} = \frac{f_{samp}}{\pi(L+1)} \arg\left\{ \sum_{k=1}^{L} R(k) \right\} \tag{5.18}$$

The mathematical expression of L is given as:

$$L = \text{round}\left(\frac{f_{samp}}{f_{max}}\right) - 1 \tag{5.19}$$

The Term R(k) in (5.18) represents autocorrelation function that can be written as:

$$R(k) = \frac{1}{N-k} \sum_{i=k+1}^{N} r_i \, r_{i-k}^{*} \tag{5.20}$$

Autocorrelation function contains two terms: $r_k$, which is the model of received signal given in (5.21), and $r_k^*$, which is the complex conjugate version of received signal given in (5.22). N symbolizes the number of samples. The term M in (5.23) is chosen as 4 since there are four possible symbols in QPSK.

$$r_k = e^{j(2\pi \Delta f k T_s + \theta)} \tag{5.21}$$

$$r_k^* = e^{-j\,(2\pi\Delta f k T_s + \theta)} \tag{5.22}$$

$$N = \frac{L+1}{M} \tag{5.23}$$

There can be rotation on the constellation diagram which is corrected in the Fine Frequency Compensation Block due to the residual frequency offsets, The digital design of CFC Block is shown in Figure 5.24.

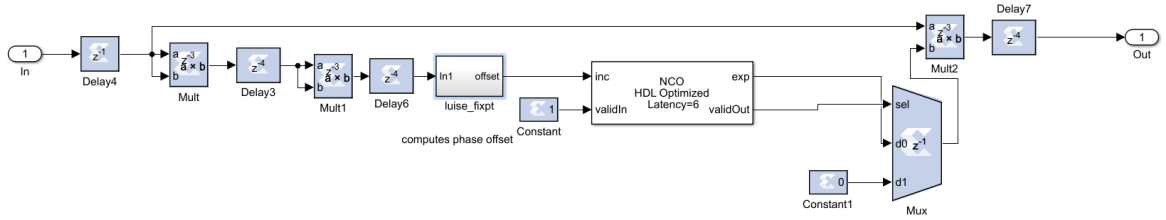


Figure 5.24: Coarse frequency compensation

### 5.2.2.3 Fine Frequency Compensation

As mentioned in the previous section, although Coarse Frequency Compensation block corrects the frequency offset, it creates a residual frequency offset which rotates the constellation. Fine Frequency Compensation (FFC) is used in Underwater 5G Technology to fix this problem. In the FFC algorithm, simply a PLL is implemented to track the residual frequency offset and the phase offset. Then as an estimator, maximum likelihood estimator is used which generates and calculates the phase error. For this purpose, a predefined MATLAB block is used. After that a Loop Filter is used to filter the calculated phase error and then phase calculation block corrects the residual frequency offset and the phase offset. Digital design of these blocks is shown on Figure 5.25, Figure 5.26 and Figure 5.27.

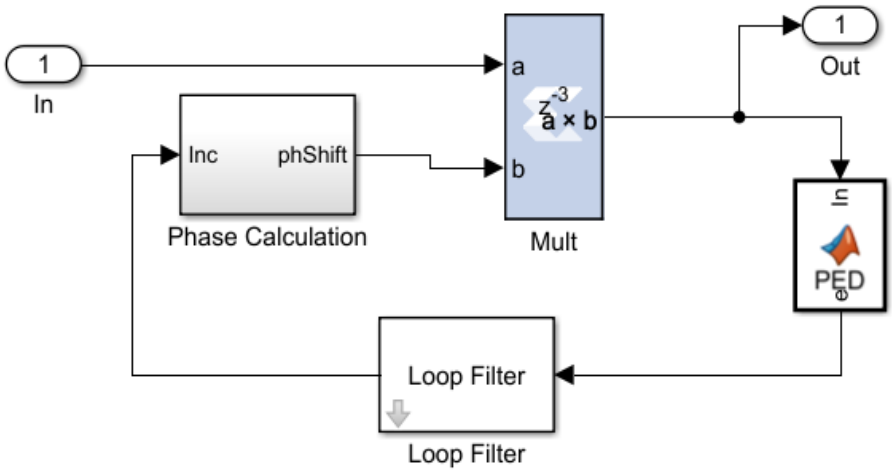


Figure 5.25: Overall Design of Fine Frequency Compensation

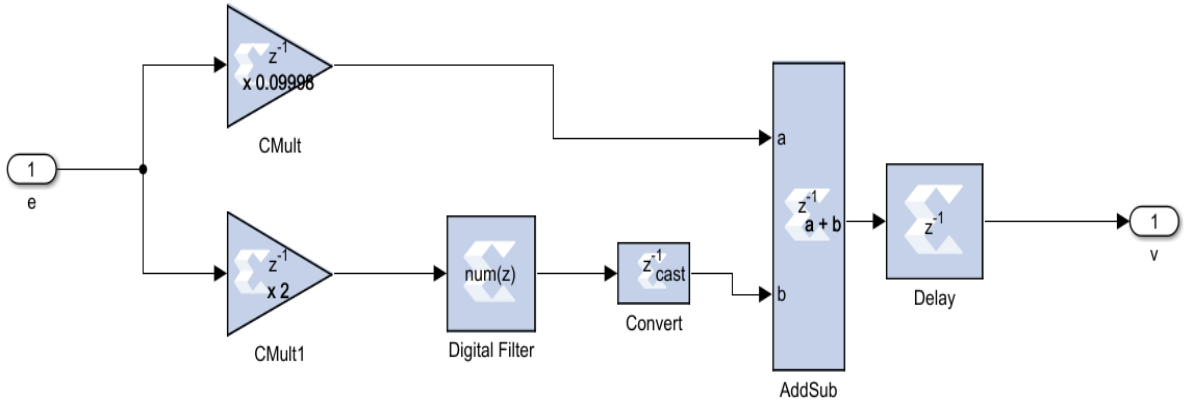


Figure 5.26: The Loop Filter

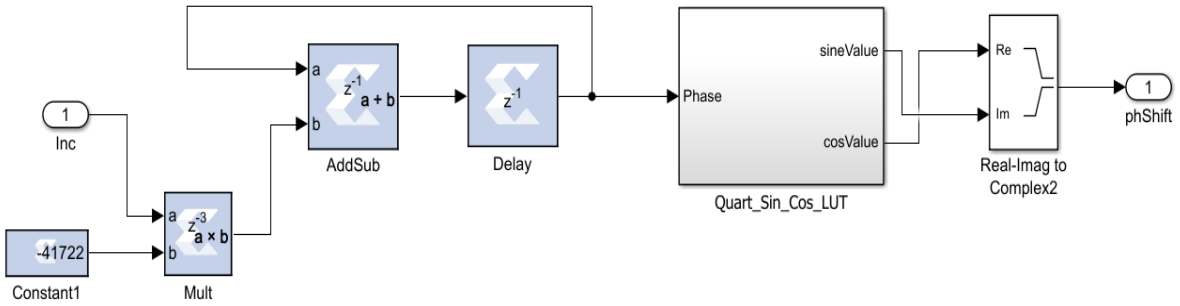


Figure 5.27: Phase Calculation

### 5.2.3 Message Decoding

After the OFDM receiving and compensation processes are done, only the digital data remains to be decoded. Message decoding includes Polar decoding, QPSK decoding and decision methodology.

#### 5.2.3.1 Match Filter

As it is explained in the transmitter part, Barker Codes are attached to the header of the message signal. Therefore, in the decoding part, the Match Filter detects the start of the signal. Match filter has a very basic digital design shown in Figure 5.28.

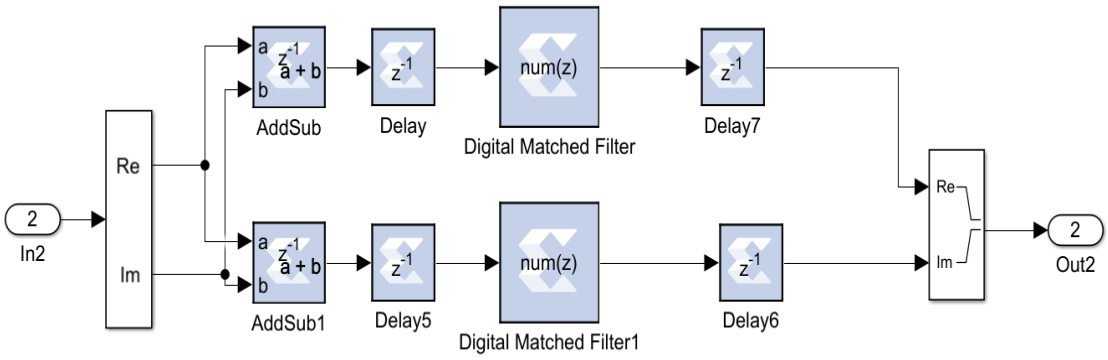


Figure 5.28: Match filter

"Digital Matched Filter" block in the Figure 5.28 is a standard FIR filter which uses a set of Barker Codes that are modulated by QPSK as a reference model for the correlation. However, Match Filter block design is not enough to calculate the correlation degree. To calculate the correlation, the equation in (5.28) must be performed.

$$\text{Correlation} = \sqrt{I^2 + Q^2} \tag{5.28}$$

Here in (5.28), I and Q symbolize the in-phase and quadrature components of the signal. It is hard to take the square root in the FPGA design, therefore to perform the task given in the above equation; the output of the match filter is connected to a "Square root" block. This block uses "$|L| + 0.4|S|$" Algorithm the details of which are given in [20]. Correlation can be approximated as:

$$|L| + 0.4|S| \quad (5.29)$$

In equation (5.29), L symbolizes the maximum value of I and Q and S symbolizes the minimum value of I and Q. After the correlation value is calculated, it is compared with a threshold value. If the output is bigger than the threshold value, the data is considered to be valid and can be demodulated. Threshold must be chosen carefully, because the small value can cause false alarm while the high value of the threshold may cause to lose the incoming signal. Barker Code length is chosen to be 26 on the transmitter side therefore threshold value must be chosen accordingly. With the help of montecarlo simulation methodology, we determined the best threshold value to be 16 for the underwater 5G technology since it prevents false alarms.

#### 5.2.3.2 QPSK Demodulation

Demodulation process of the signal is relatively easier than the modulation process. For the QPSK demodulation, since the symbols are already in base band, there is no need for operations such as carrier synchronization. The only objective is to make predictions based on base band symbols. For this purpose, FIR filter is used. The FIR filter is designed on FDA tool of System Generator.

Window function design technique is used for the Low-pass filter design of QPSK demodulator. The window function design method basically selects the desired filter with the ideal frequency characteristics. Then, it truncates its impulse response to generate a Low Pass filter of linear-phase. Impulse response of the designed filter is shown in Figure 5.29.

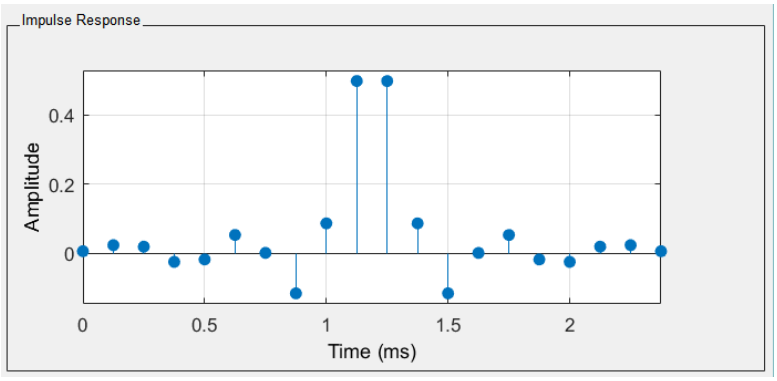


Figure 5.29: Impulse response of LPF

After the filter is designed, the output symbols are predicted. For this prediction, there are two commonly used decision theorems in the literature which are Soft Decision and Hard Decision. In information theory, Soft Decision methodology, the incoming data is decoded by considering a list that consists of possible decoded values of the data. Although this decision theorem may result in better bit error rates, it increases the complexity of the design. In this thesis, we used Hard Decision theorem which simply compares the incoming data with the candidate outputs and checks the hamming distances among them. Most similar candidate output is decided to be final decoded data.

#### 5.2.3.3 Polar Code Decoding

Although it is relatively easy to encode the data with Polar Codes, it is difficult to decode. There are only XOR operators in the Encoder while there are many other operators in the decoding part.

Successive Cancellation Decoder algorithm is proposed by Erdal Arikan for the first time [20]. Basically, the decoding process starts from the right hand side of the graphical representation of the encoding in Figure 5.4, from right to left and from bottom to the top sequentially. It successively tries to estimate $\widehat{u_k}$ from the channel outputs. Graphical representation of SC Decoding is shown in Figure 5.30.

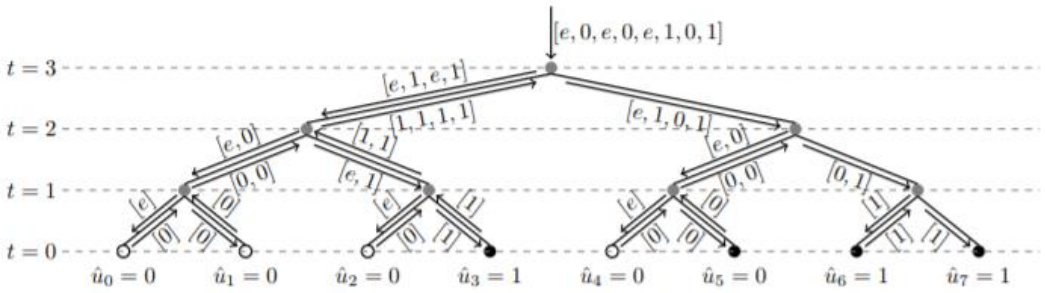


Figure 5.30: SC decoder

Successive Cancellation List Decoder (SCL) Algorithm has many similarities in terms of the algorithm with Successive Cancellation (SC) Algorithm with a significant difference which is the generated list. SCL algorithm generates a list of "L" which holds candidate code words. Candidate code words are chosen from the values of $\widehat{u_k}$ for the

information bit locations. From the beginning of the calculation, only the determined number of best paths survives and the others are neglected. At the end of the calculation process, best path is chosen from this list and it is served as a decoded bit. For the underwater 5G Technology, SCL Decoder is chosen to be the Polar Decoding algorithm because it gives better results than SC decoder as stated in [22]. representation of SC against SCL decoder is shown in Figure 5.31. As shown on the graphical representation, while the SC chooses one path, SCL decoder holds a list of possible paths. Bit error rate decreases with SCL decoder with the help of this list.

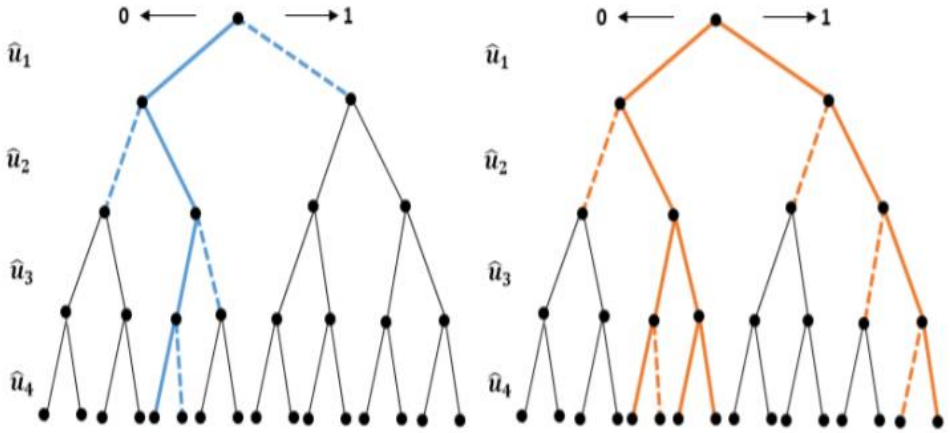


Figure 5.31: “a) SC decoding. b) Successive cancellation list (SCL) decoding (list size L = 4). Bold face lines are Inspected paths.”[22]

## 5.3 Acoustic Channel Model

Complete design of Underwater 5G Technology is given in the previous sections. To measure the performance of this system before the hardware implementation, an acoustic channel model is implemented. For the best performance of the system, acoustic channel model must be realistic. Acoustic channel model is generated with three main parameters: Attenuation, Noise and Multipath Effects.

### 5.3.1 Attenuation

Bit rate is the data transfer rate per second that can be transmitted along a digital network. This is also termed as Channel Capacity. The channel capacity increases while the communication frequency is increased. However, the usable frequency in acoustic communication is limited due to attenuation. As the frequency increases, the attenuation

also increases. Beyond a frequency, the penetration of the acoustic waves into the water becomes very poor when the communication stops.

In acoustic communication, the attenuation of the signal not only depends on the distance but also depends on the speed of the sound waves in the water. Although inconsistent, the sound speed in water is accepted as 1500 m/s. The Sound Speed under the water depends on several characteristics of water such as the depth, salinity, temperature and Ph value. Apart from these characteristics, the speed also depends on the distance and the communication frequency.

The factors of the attenuation are well known. However, there is not any scientific formula to calculate the attenuation. There are empirical formulas proposed by Ainsline & McColm [26] which gives an accurate estimation about the attenuation of the acoustic waves. These attenuations are mathematically expressed by the Eq.5.30-5.35 .

$$B = 0.78\sqrt{\frac{S}{35}}\, e^{\frac{T}{26}} \tag{5.30}$$

$$Mg = 42e^{\frac{T}{17}} \tag{5.31}$$

$$a_1 = \frac{B \times 0.106 \times f^2 \times e^{\frac{Ph - 8}{0.56}}}{B^2 + Mg^2} \tag{5.32}$$

$$a_2 = 0.52 \times \left(1 + \frac{T}{43}\right) \times \left(\frac{S}{35}\right) \times \left(\frac{f^2 * (Mg^2) * \exp\left(-\frac{D}{6}\right)}{Mg^2 + f^2}\right) \tag{5.33}$$

$$a_3 = 0.00049 \times (f^2) \times \exp\left(-\left(\frac{T}{27} + \frac{D}{17}\right)\right) \tag{5.34}$$

$$\text{Sound Absorption} = a_1 + a_2 + a_3 \tag{5.35}$$

In equation (5.30), B symbolizes the Boric Acid and in equation (5.31), Mg symbolizes the Magnesium Sulfide. Term T represents temperature in terms of Celsius, D represents depth in meter, S represents salinity in parts per thousand (ppt), Ph represents ph value of the sea or ocean and f is the frequency in kHz.

If the wave is spherical which means depth of the sea or ocean is bigger than the transmission range:

$$TL = 20 \times \log_{10} 1000R \quad (5.36)$$

If the wave is cylindrical which means depth of the sea or ocean is smaller than the transmission range:

$$TL = 10 \times \log_{10} 1000 {}^{D}/_{2} + 10 \times \log_{10} 1000R \quad (5.37)$$

Finally, from the equations (5.30) to (5.37), attenuation can be calculated as:

$$\text{Attenuation} = TL + (a_1 + a_2 + a_3) \times R \quad (5.38)$$

In equations (5.36) to (5.38), TL means transmission loss and R symbolizes the distance in kilometer.

### 5.3.2 Noise

To find the maximum channel capacity, the relation between the transmitter and the receiver must be well-defined. For a successful communication, transmitted signal must be received with an acceptable noise level to be interpreted correctly, which depends on the SNR of the signal. Then, modeling of the noise underwater becomes an important issue.

"The ambient noise in the ocean can be modeled by using four sources: turbulence, shipping, waves, and thermal noise. Most of the ambient noise sources can be described by Gaussian statistics with a continuous power spectral density. Noise modeling for underwater is given in [22]. However, there are no scientific equations to calculate these noises. Therefore, all the given equations are empirical. In this thesis, it is assumed that the communication will occur in deep water. Therefore, the noise can be considered as white noise.

Additive White Gaussian Noise (AWGN) model is used for the ambient noise model of the underwater 5G technology. There are three main parameters for the AWGN which are:

- Signal to Noise Ratio (SNR),
- Bit Energy to power spectral noise density ratio ($\frac{E_b}{N_0}$),
- Symbol Energy to power spectral noise density ratio ($\frac{E_s}{N_0}$).

The relation between $\frac{E_b}{N_0}$ and $\frac{E_s}{N_0}$ can be written as:

$$\frac{E_s}{N_0}(\text{dB}) = \frac{E_b}{N_0}(\text{dB}) + 10\log_{10}2 \tag{5.39}$$

Signal to Noise Ratio (SNR) can also be given in terms of $\frac{E_s}{N_0}$ as:

$$\text{SNR(dB)} = \frac{E_s}{N_0}(\text{dB}) - 10\log_{10}\left(\frac{T_{sym}}{T_{samp}}\right) \tag{5.40}$$

$$\text{SNR(dB)} = \frac{E_s}{N_0}(\text{dB}) - 10\log_{10}\left(\frac{0.5T_{sym}}{T_{samp}}\right) \tag{5.41}$$

Equation (5.40) is defined for complex input signals and equation (5.41) is defined for real input signals.

### 5.3.3 Multipath Effects

Acoustic waves under the water do not follow a linear path [1]. The characteristic of water such as temperature and density is different at different depths. Therefore, as the acoustic waves travel through water. Some of the incident wave refracted and some of them is reflected back from the surface or from another layer of water. This reflection is shown in Figure 5.32.

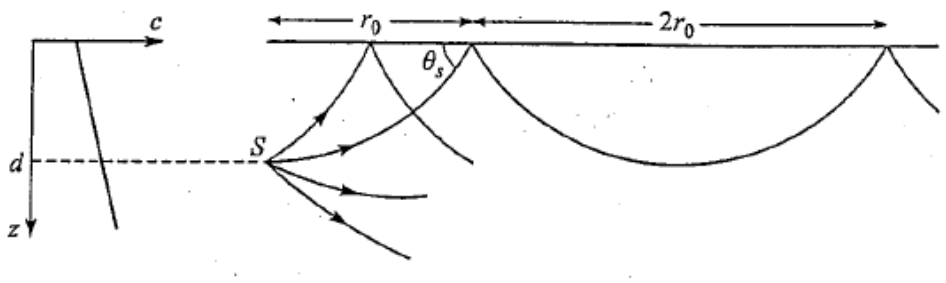


Figure 5.32: Bouncing incident waves [1]

As you see in Figure 5.32, after the incident wave is sent from the source (depicted as “S” on Figure 3.1), it hits the surface for a second time after it travels some amount of distance . This phenomenon causes receiving multiple copies of the original message at the receiver side and this effect is called “Multipath Effect”.

One of the most challenging problem in underwater acoustic communication is the multipath effect. Multipath propagation of the incident wave causes time variant corrupted length path to the receiver. Underwater communications shows that arrival of the time-variant multipath signals to the receiver sides creates a huge complexity for the signal to be interpreted precisely. To communicate over a certain amount of distance, at the receiver side, multipath effects of the original signal must be eliminated; otherwise a clear communication cannot be established.

At the receiver side, different designs can be implemented to eliminate multipath. However, these designs increase complexity which in turn decreases the applicability of the system. In this thesis, underwater 5G technology is proposed to eliminate the so-called Multipath Effect.

Transmitted baseband signal x[n] is defined in equation (5.5) previously. Based on the transmitted signal in (5.5), the received signal r[n] can be re-written as:

$$r[n] = \sum_{k=0}^{N-1} \rho_k[n] \cdot a(n- \tau_k[n]) \quad (5.42)$$

Here in (5.42), the $\rho_k[n]$ is the $k_{th}$ attenuation and the $\tau_k[n]$ is the delay on the received signal. Acoustic signals in underwater follows ray paths and many multipath effects as stated in the (5.42) are delivered to the receiver. Therefore, the UWA channel behaves like there are many reflectors between transmitter and the receiver. For such environments, it is reasonable to use Rayleigh Multipath Fading Channel Model.

When there are many ray reflections, each ray chooses a different path to be reflected. Each path of the Rays can be modeled as “A Circularly Symmetric Complex Gaussian Random Variable” (CSCGRV) time-variant system. The CSCGRV has the form in (5.43) .

$$Z = X + jY \tag{5.43}$$

Here , X and Y are the Gaussian random variables which are independently and identically distributed with zero mean. Therefore, for the term Z which is a circularly symmetric complex random variable, the statement can be re-written as in (5.44).

$$E[Z] = E\left[e^{j\Theta} Z\right] = e^{j\Theta} E[Z] \tag{5.44}$$

The variance of the system is:

$$\sigma^2 = E[Z^2] \tag{5.45}$$

The magnitude of Z is known as “A Rayleigh Random Variable” whose probability density function can be represented by Eq. (5.46).

$$p(z) = \frac{z}{\sigma^2} e^{-\frac{z^2}{2\sigma^2}}, \quad z \geq 0 \tag{5.46}$$

This channel model is called Rayleigh Fading Channel Model and it is selected as UWA channel model for the simulation of underwater 5G technology.

### 5.3.4 Simulation of Acoustic Channel Model

Underwater Acoustic channel model must include all the properties which are attenuation, noise and multipath effects. For the attenuation model, two cases are generally evaluated. In first case, all paths on the sub-channel have random attenuations except from the first path which has a constant attenuation and phase [23]. For this first case, Rician channel is used. In the second case, any path on sub-channel has random attenuation. Their occurrences are constant during symbol duration [23]. For this second case, Rayleigh channel is used. Except from the attenuations, Rayleigh and Rician fading models have multipath effects which make them suitable for our design. For the UWA acoustic channel, Rayleigh Fading model is decided to be used to simulate Fading Multipath Effects with random attenuations and AWGN is chosen to simulate ambient noise. For this purpose, predefined MATLAB blocks are used. The UWA channel model is shown in Figure 5.33.

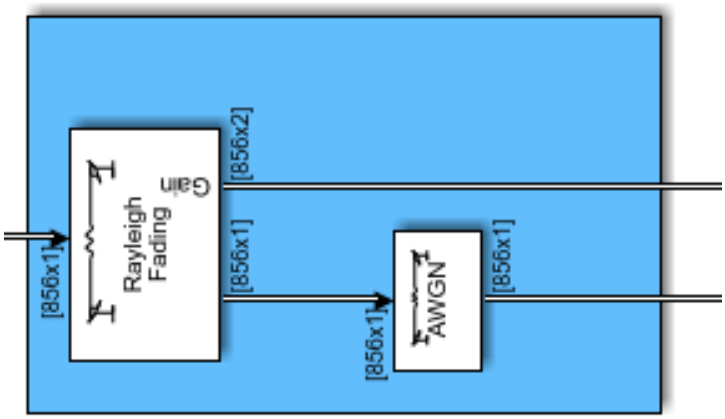


Figure 5.33: UWA channel model

Impulse response of the UWA channel is shown in Figure 5.34. Red impulse shows the actual data and blue one shows the output of the channel. The delay and multipath effects are randomly created within the channel.


Figure 5.34: Impulse response of the multipath channel

Scattering, multipath fading components and Doppler spectrum are shown in Figure 5.35, Figure 5.36 and Figure 5.37.

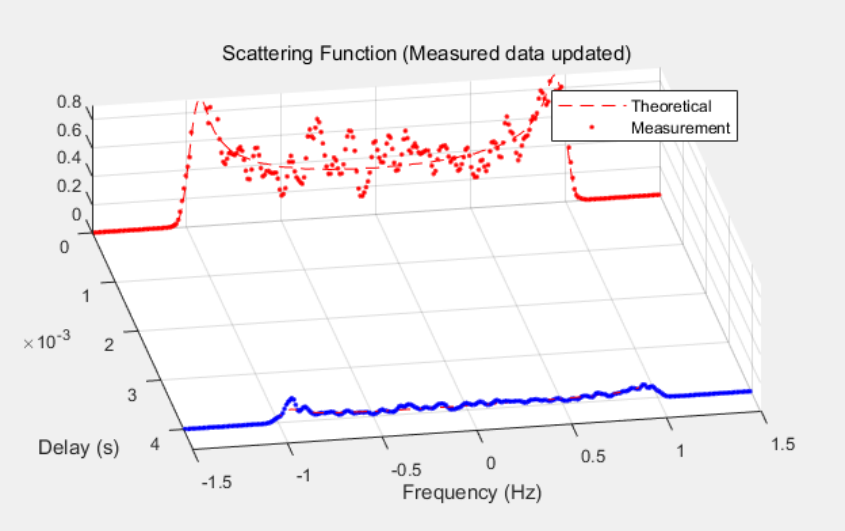


Figure 5.35: Scattering function

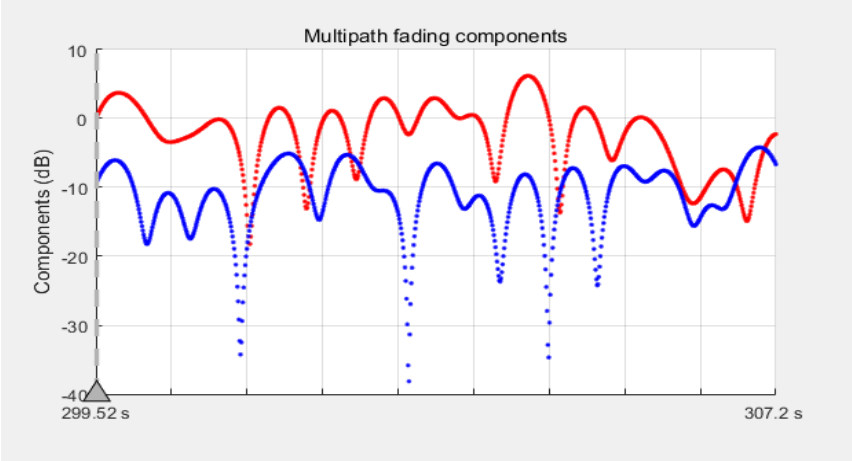


Figure 5.36: Multipath components

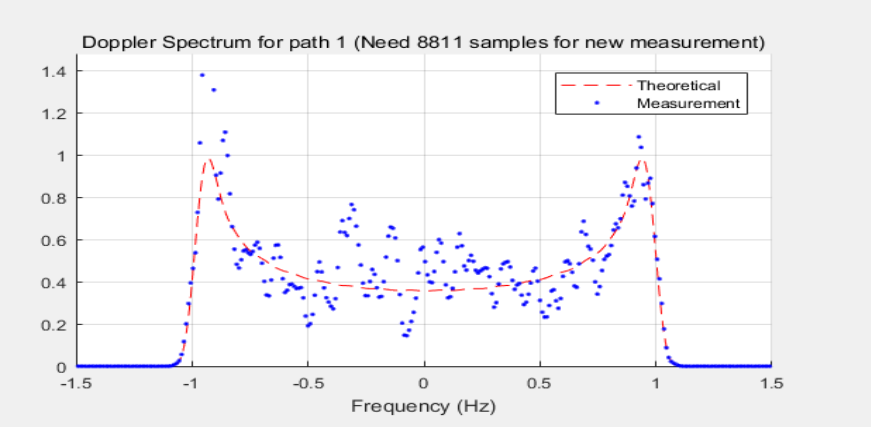


Figure 5.37: Doppler spectrum

To increase the reality of the channel, a very noisy channel is created with many multipath effects. Amplitude of the multipath effects and their delays are randomly created. The spectrum of the OFDM Signal before the channel is shown in Figure 5.38. The channel output is shown in Figure 5.39.

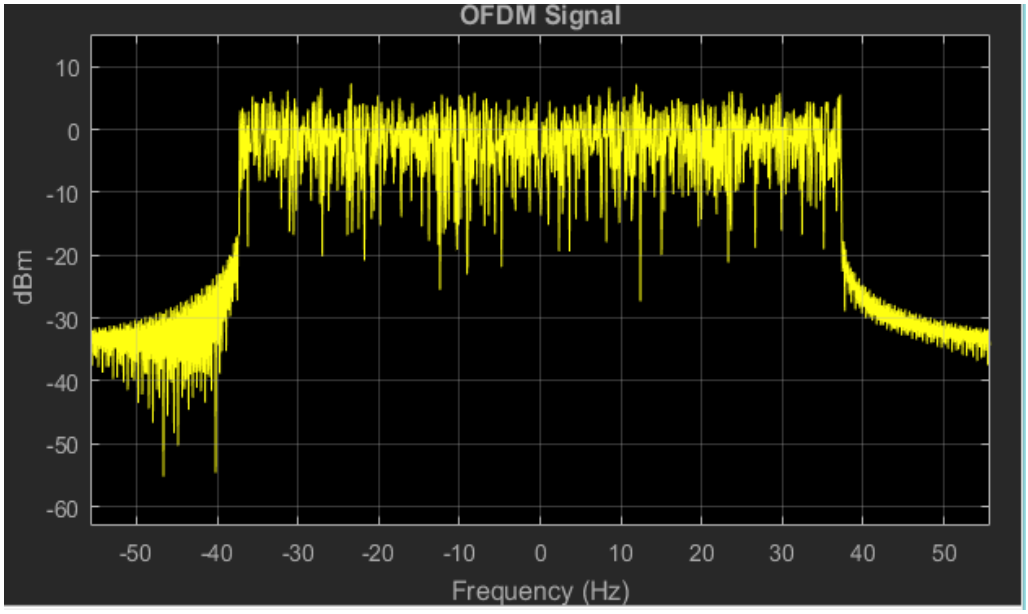


Figure 5.38: OFDM signal spectrum

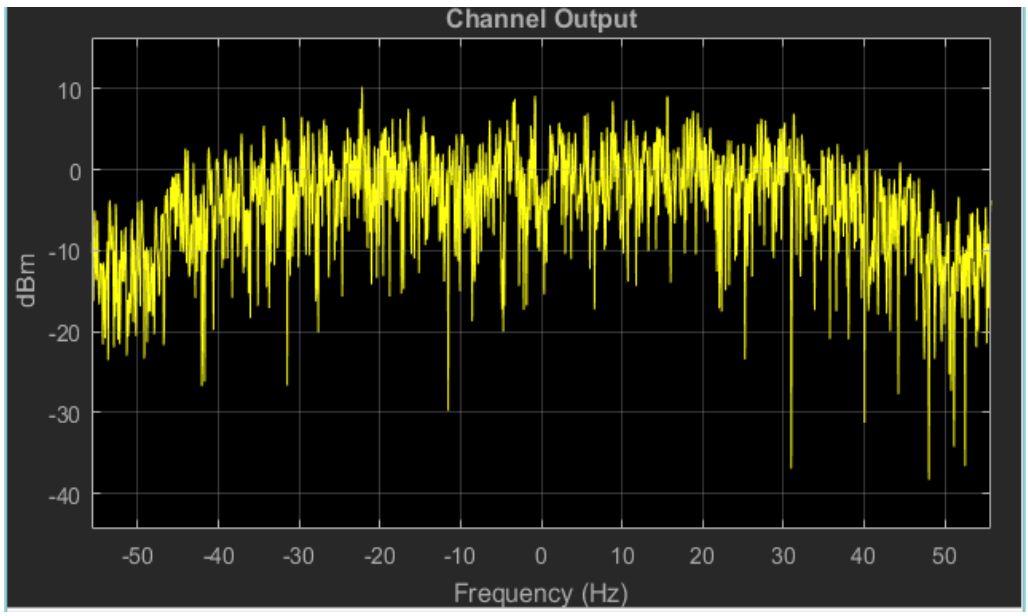


Figure 5.39: UWA channel output

# 6. HARDWARE DESIGN

In this thesis, the main concentration is on the digital design of the system. However, we found it useful to design also the hardware so that we can prove our digital design in a test environment.

## 6.1 Transmitter Design

The hardware design of the transmitter consists of four basic elements. First one is the FPGA. As mentioned above, all the designs are made so as to work in a FPGA. Xilinx's ZYNQ-7020 is chosen for symbol creation and signal generation. The IP that is created via MATLAB System Generator is added into ZYNQ Design on Vivado Software. This IP directly takes the incoming data and converts it to OFDM symbols. After that the symbols are sampled to the PMODs of the FPGA as 16 bit output.

After the OFDM symbols are generated, the signal is converted to Analog with a DAC (Digital to Analog Converter). As our system works at slow data rates such as 20 kHz to 100 kHz, the sampling frequency of the DAC doesn't have to be so high. However, to sample the system good enough, the DAC is chosen to be 1 Ms/s (Mega sample per second) which is quite satisfactory for the proposed system. The SPI control code of the DAC is also written on the FPGA.

The last two parts of the transmitter system are the Power Amplifier and Transducer parts. Transducer converts the analog signal to acoustic waves and the Power Amplifier amplifies this signal to propagate farther. The amplifier and the transducer can be designed separately. However, there are many commercial products that serves 2 in 1 system which includes both the amplifier and the transducer. For the underwater 5G Technology hardware test, 2 in 1 system is used. Therefore, the transducer has an adjustable gain range from 0 to 60 dB.

## 6.2 Receiver Design

The Receiver's hardware design also consists of four elements. The first one is the receiving part of the incoming acoustic signals. The incoming acoustic waves reach the receiver with very low voltages in the order of millivolts. To receive these signals, Pre-amplifier is used. Pre-amplifier's working principle is the same as Low Noise Amplifier

(LNA) which is used for RF communication, both tries to amplify the signal without amplifying the ambient noise. So, the incoming signal is amplified first with pre-amplified and then converted from acoustic waves to analog signal by Hydrophone.

After the signal is captured, the next process is to convert this signal from analog to digital with an ADC. The sampling frequency of the ADC is chosen to be the same with DAC as 1 Ms/s. SPI controller code of ADC is written in FPGA.

In the last stage, the received data is converted to the digital data of OFDM symbols to raw data. This process is performed in the FPGA design. The IP design that is created on MATLAB with System Generator is directly added to ZYNQ design.

# 7. RESULTS

## 7.1 Simulation Results

Digital Design of the blocks shown in Figure 5.1 are implemented to compose the complete transceiver design. The final stage of the simulation for underwater 5G technology is the performance evaluation part. The Transmitter and the Receiver of the system are connected by an acoustic channel and they are connected to a bit error rate calculation block. The overall design is shown on Figure 7.1.

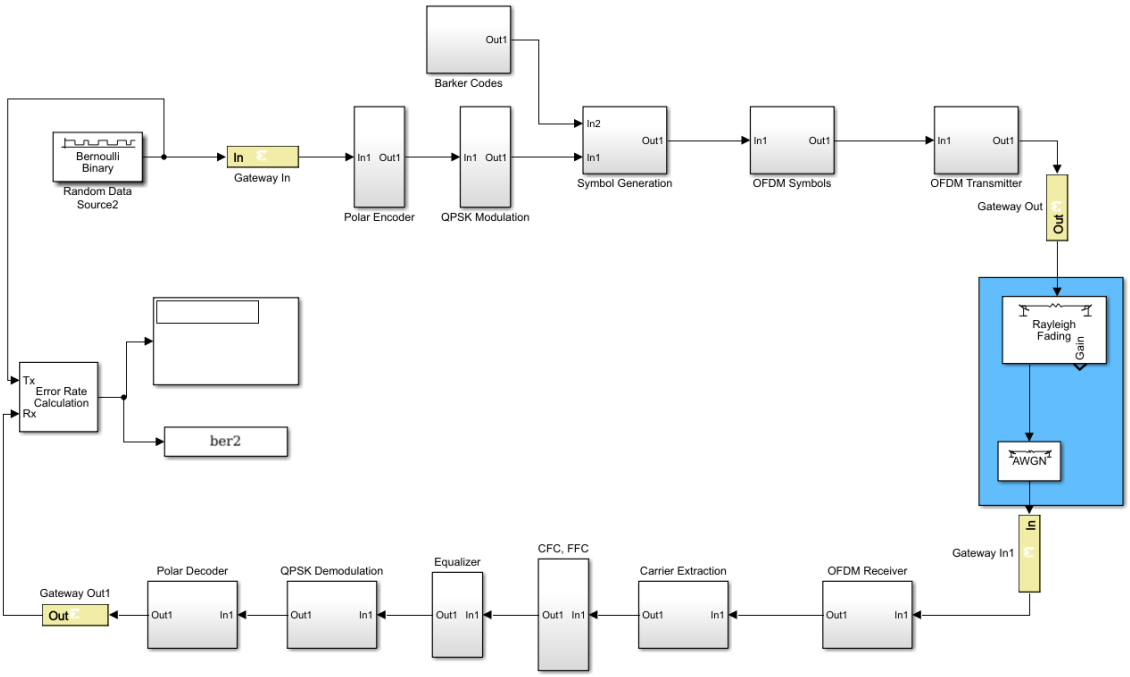


Figure 7.1: Overall simulation

To discuss the performance of the receiver, the constellation outputs of some important blocks are evaluated below. Channel output and equalization process are shown in Figure 7.2. As it is shown, noisy data comes out of the channel. After the carrier extraction, the symbols are scattered to the diagram. However, it is a normal phenomenon because there are hundreds of symbols in OFDM modulation scheme. After the carrier extraction processes, the Equalizer estimates the channel successfully and corrects the constellation diagram.

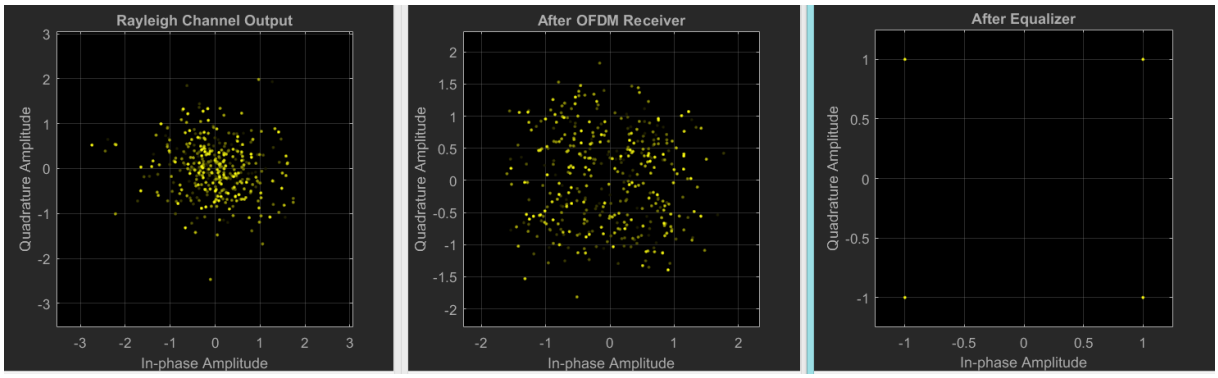


Figure 7.2: Constellation diagrams of a) Rayleigh channel output b) OFDM receiver output c) Equalizer output

Although in part c of Figure 7.2 looks like correct, the symbols don't represent the real values. For this purpose, compensation processes were carried out and the output of that processes are shown on Figure 7.3. As it is explained above, after the Coarse Frequency Compensation, a rotation occurs in constellation diagram. To fix this issue, Fine Frequency Compensation was used. Final constellation diagram are shown on part b of Figure 7.3.

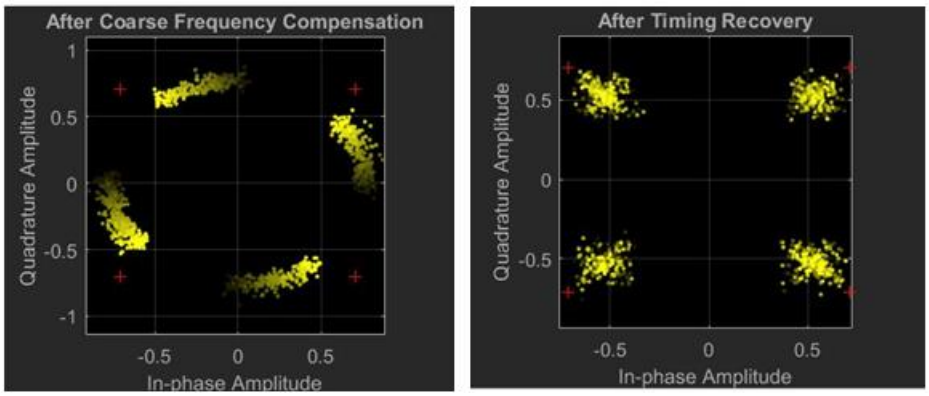


Figure 7.3: Compensation processes a) Coarse frequency compensation b) Fine frequency compensation

There are many adjustable parameters for the proposed system such as FFT Length for OFDM, the type of QPSK modulation, Guard Band Timing, Barker code length, Scrambler's polynomial and etc. All of these can be re-adjusted which causes many cases that must be compared with each other. In this thesis, as an optimal design and for the sake of achieving a meaningful conclusion, all parameters are fixed except the Polar

Code Rate that indicates the ratio of information bits to total number of bits and the Cyclic Prefix rate that indicates the portion of the transmitted signal added to its tail as a cyclic prefix. The bit error rates graph for the Underwater 5G Technology for different Polar Code and CP rates are shown on Figure 7.4. Monte-Carlo methodology is used for the simulation. The other fixed parameters are shown in Table 7.1.

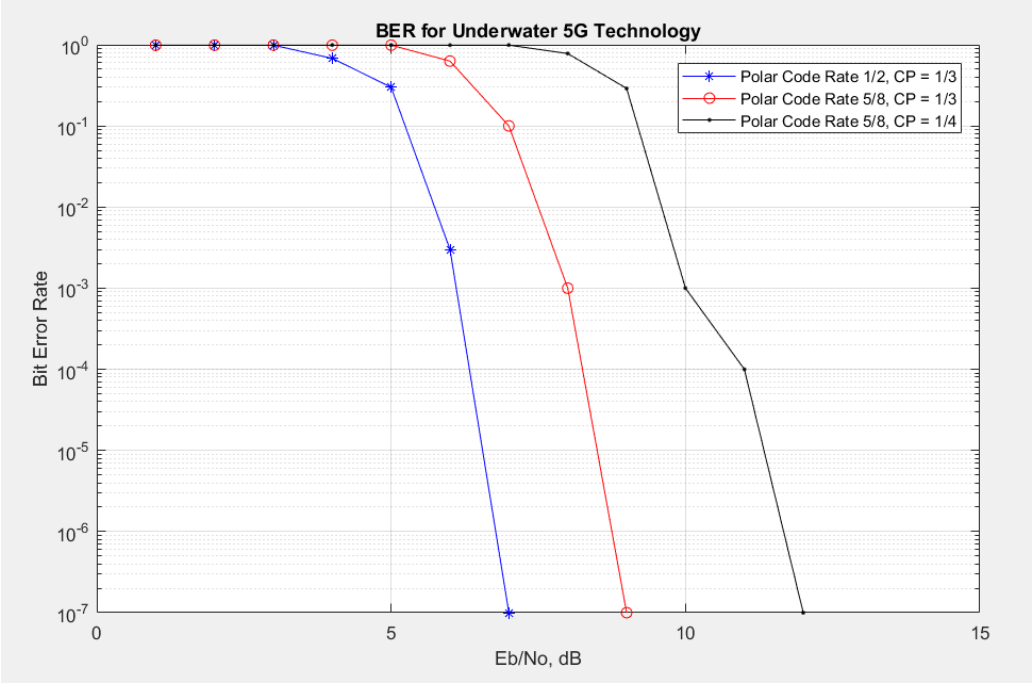


Figure 7.4: Bit error rate of the underwater 5G technology

Table 7.1. Underwater 5G Technology Parameters

| **Parameter Definition** | **The value of the Parameter** |
|---|---|
| Frame Length | 1024 bits |
| CP Rate | 1/3 & 1/4 |
| Polar Code Rate | 1/2 (512 bits) & 5/8(640 bits) |
| Modulation Type | OFDM |
| Symbol Generation | QPSK |
| Transmission Frequency | 20 kHz-30 kHz |
| Guard Band Time | 20 ms |
| Preamble | 26 bit Barker Code |
| Data Rate | 30Kbps to 60Kbps |

The rate of the Polar Code determines the entropy of the communication. When the rate is 1/2 it means that only half of the transmitted signal includes the information and the other half is predetermined frozen bits. The system operates between 30 Kbps to 60 Kbps which is considered as a moderate data speed in the literature. Therefore this kind of polar code rating with this data rate is acceptable. Therefore, the BER graph which is shown in Figure 7.4 indicates that Underwater 5G Technology works very well. The blue line of the graph which symbolizes the communication with a Polar Code Rate of 1/2 shows that the underwater communication can start when the Eb/N0 rating is approximately 5 dB which is a very noisy channel. Although the communication starts at nearly 5 dB, the best performance of the transaction is achieved at 7 dB Eb/N0 rating. This result shows that after the communication is started, even if it is very noisy environment, the end to end Underwater 5G Technology rapidly recovers the data which is exposed to heavy noise and the system offers the end users a clear communication.

## 7.2 Test Results

To test the system's feasibility and to examine the simulations' results, Underwater 5G Technology's test experiment was conducted at an acoustic tank operated by TR ARGE Company, Turkey.

Although the Underwater 5G Technology aims at working at deep waters, the shallow water tank experiment gives realistic results because there are more multipath and scattering effects in the shallow water than deep water. This indicates that if a system can establish a communication in shallow water, generally it establishes a better communication in deep water since deep water channel is better in terms of multipath and scattering effects

For this experiment, a transducer and hydrophone was located at two different location of the water tank shown Figure 7.5. The transmitter was located at 10 m depth and the receiver located to 12 m horizontally away from the transducer and at 5m depth. The test was conducted with the parameters in Table 7.1. Polar Code Rate was chosen as 1/2 and Cyclic Prefix length was 1/3 of the transmitted signal.

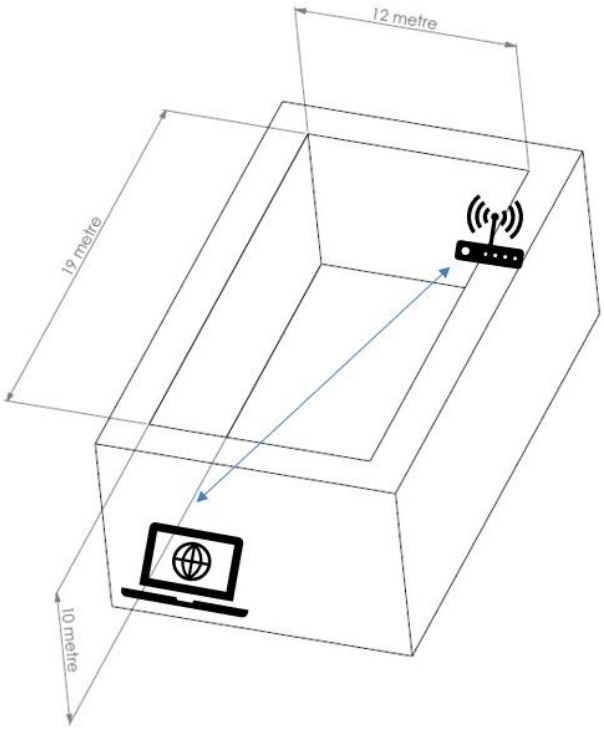


Figure 7.5: Water tank

To test the Bit Error Rate, ASCII Code of "Hello World" was sent to the receiver. The received symbols were saved to a block memory. Then, with the support of MATLAB, the bit error rate was calculated. For the test duration, 100 "Hello world" messages were sent, and they were received with $1x10^{-5}$ Bit error rate. Bit error rate is consistent with the simulations. However, to discuss the performance of the system, the SNR of the acoustic channel must be known. The measurements showed that SNR of the acoustic channel was nearly 8.73 dB. Therefore, we can confidently state that Underwater 5G technology works with low bit error rate in noisy channels as expected from simulations.

To examine the test results, SNR of the acoustic channel was measured with the same test setup. For the SNR measurement, a pure sinusoidal signal was transmitted across the channel. Then the power spectral density of the received signal was examined. The incoming impulses except from the actual signal are called Noise-Floor (NF). The Noise-Floor provides enough information to calculate SNR. For this calculation the following equation was used [27]:

$$SNR_{min} = SL - NL + DI - TL \quad (7.1)$$

Here in (7.1), SL symbolizes the source level which is the radiated pressure level relative to 1 μPa measured at 1 m away from the source. NL symbolizes the noise level which is the additional received energy caused by outside environmental events. Higher NL makes the signal harder to detect. DI represents the directivity index, ability of the transducer to physically or electronically direct its received response in space, and TL represents the transmission loss.

As the sensitivity of the hydrophone in the receiver side is known, the SNR was calculated as nearly 9.73 dB.

For the comparison, an UWA communication system which uses Turbo Codes for the FEC methodology has reached 2.8kbps to 9kbps with 10-4 BER [25], while our proposed Underwater 5G Technology system has reached 30kbps to 60kbps with 10-5 BER. On the other hand, in the literature, Polar Codes with OFDM is used for UWA Communication systems [11]. Although they don't present an end to end system, they have used OFDM and Polar codes in the physical layer. They have reached $10^{-7}$ BER while the SNR was 17 dB with a polar code rate of 7/16 [11], while our system can reach this BER with 6 dB SNR with the 1/2 polar code rate, which means our system performs better in a worse SNR environment with a better rating of the polar codes. The comparison is shown on Figure 7.6 "Design A" symbolizes our proposed design and "Design B" symbolizes the compared design [11]. It can be easily recognized that our system not also starts sensing the incoming signal earlier but also it performs better in low SNR.

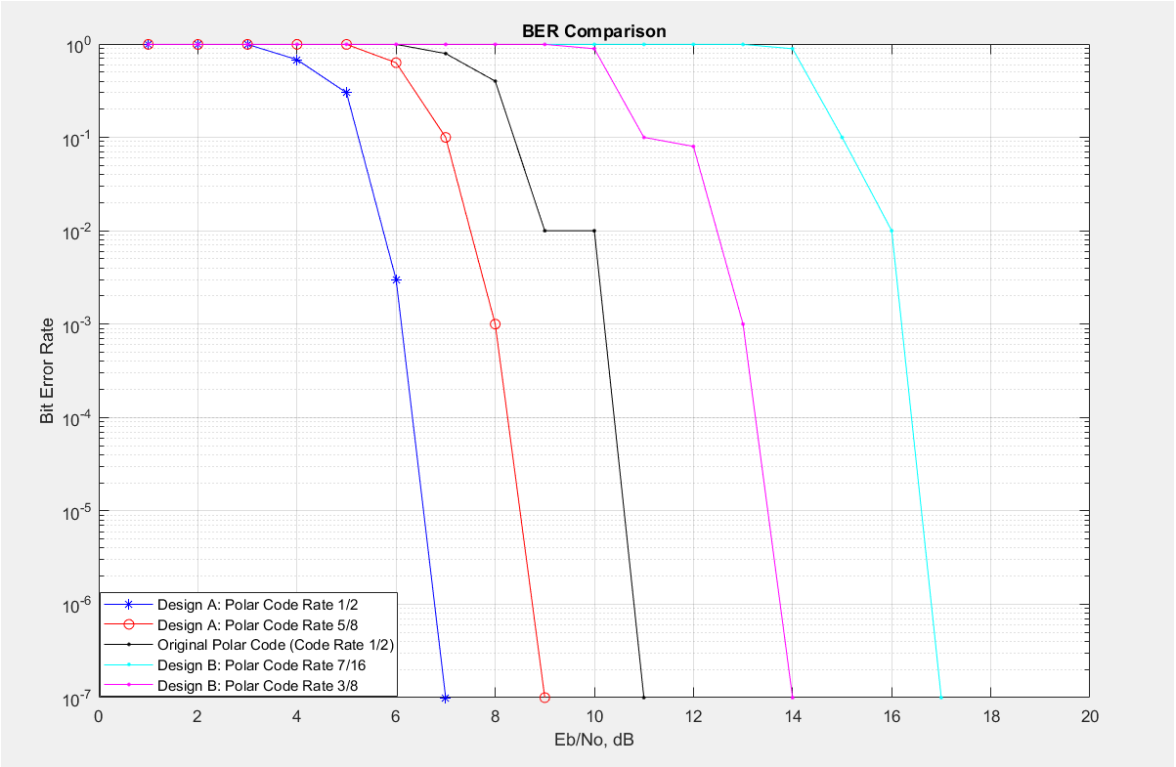


Figure 7.6: Comparison of Designs

# 8. SUMMARY

In this thesis, we have presented a complete end-to-end underwater acoustic communication system which operates in real time. Since this system combines the physical layer of 5G technology with known acoustic communication techniques, we called it underwater 5G technology. Underwater 5G Technology aims at maintaining a robust underwater communication link by overcoming the two main obstacles, Scattering and Multipath. For this purpose, a complete digital design is proposed in this thesis. Designed transmitter and receiver include all the necessary modules for a reliable underwater communication. This communication is called as underwater 5G communication because it imitates all the necessary parts of RF 5G Technology successfully.

To imitate 5G RF technology, most important parts for data link layer are used which are Polar Codes and OFDM modulation scheme. Then, these two are combined with modern communication techniques which are suitable for underwater technology such as scrambling and barker codes. After a fine communication link is established with the proposed digital designs, the receiver techniques for underwater technology is used which includes Zero-Force Equalizer to recover the incoming message symbols. Finally, to discuss the performance of the system, a channel model is designed.

Performance evaluation is carried out on the final part by comparing the test results with the simulations. The transmitter is connected to the receiver via an acoustic channel model. Although there are many adjustable parameters for the performance comparison, two modules dominantly affects the bit error rate of the system, Polar Code Rate and the length of Cyclic prefix. It is clearly shown that while the CP length increases and Polar Code Rate decreases, the performance of the system increases. Apart from these parameters, there are other parameters that affect system performance such as the offset of the QPSK. For the underwater 5G Technology, $3\pi/4$ OQPSK is used as sub modulation technique because it improves BER as 0.04 compared to standard QPSK. According to these adjustable parameters, Bit Error Rate graph is given. From the given BER graph which is shown in Figure 7.4, it is indicated that system can operate with very low SNR with different configurations.

To prove and double check the simulation results, a tank experiment is carried out. In the tank experiment, SNR is measured and it shows that simulations are consistent with the design. It is expected to be consistent because all the digital design is directly converted to IP and embedded to the FPGA design. Test results show that Underwater 5G system can establish a robust acoustic link in low SNR.

To sum up, as the novelty of the system, we have both cleared how to use most known modules of an acoustic communication system and how to implement these to a FPGA such as modulator, scrambler, error correction algorithms, equalizer and etc. We established an end to end system design for Underwater 5G Technology. Our system not only establishes a reliable communication between transceivers but also shows that in terms of BER and Data rate, it is superior to other designs in the literature.

# 9. FURTHER RESEARCH

In this thesis, we generally focused on to make improvements in data link layer of the communication and to develop novel algorithms in this layer to establish a reliable end to end communication system. However there are other layers which can be also improved.

For further research areas and developments of presented Underwater 5G Technology, one can apply state of the art hardware design techniques such as creating a hydrophone array on the receiver side to acquire MIMO technology. When the hydrophone array is constructed by an appropriate design, better BER and Data Rate may be achieved.

Apart from the hardware design, there can be some modifications on network layer. Automatic repeat request (ARQ) can be implemented to the channel estimation part. ARQ is an error control mechanism that simply uses acknowledge messages during data transmission. When ARQ is implemented, the system may be more reliable with less bit error rate.

Finally, other channel estimation methodologies and adaptive modulation schemes which changes according to the SNR level can be implemented for our Underwater 5G Technology design. The base design of our system can establish a reliable end to end communication, and the candidate modulation schemes and channel estimation methodologies may help to increase the data rate of the system.

# REFERENCES


[1] F. Norman, B. Andrew D., W. Jonathan, P. Clifford T. and T. Maurice, "An integrated, underwater optical/acoustic communications system", IEEE, 2010. (doi:10.1109/OCEANSSYD.2010.5603510)

[2] K. Daniel B. and B. Arthur B., "The state of the art in underwater acoustic telemetry", IEEE Journal of Oceanic Engineering, vol.25, p.4–27, 2000. (doi:10.1109/48.820733)

[3] S. Milica, "Recent Advances in High-Speed Underwater Acoustic Communications", IEEE Journal of Oceanic Engineering, vol.21, p.125–136, 1996. (doi:10.1109/48.486787)

[4] F. Lee, S. Milica, K. Daniel and P. James, "High-Rate Phase-Coherent Acoustic Communication: A Review of a Decade of Research and a Perspective on Future Challenges", In Proc. 7th European Conf. on Underwater Acoustics, 2004.

[5] R. Andreja, A. Rameez, D. Tolga M., P. John G. and S. Milica, "Adaptive OFDM Modulation for Underwater Acoustic Communications: Design Considerations and Experimental Results", IEEE Journal of Oceanic Engineering, vol.39, no.2, pp 357-370, 2014. (doi:10.1109/JOE.2013.2253212)

[6] S. Ethem, S. Milica and P. John G., "Underwater Acoustic Networks", IEEE Journal of Oceanic Engineering, vol.25, p.72–83, 2000. (doi:10.1109/48.820738)

[7] A. Ian F., P. Dario and M. Tommaso, "Underwater acoustic sensor networks: research challenges", Elsevier, Ad Hoc Networks, vol.3, p.257-279, 2005. (doi:10.1016/j.adhoc.2005.01.004)

[8] H. John, Y. Wei, W. J., S. Affan A. and L. Yuan, "Research Challenges and Applications for Underwater Sensor Networking", In Submitted to Proc. IEEE

Wireless Comm. and Networking Conf., 2006. (doi:10.1109/WCNC.2006.1683469)

[9] C. Jun-Hong, K. Jiejun, G. Mario and Z. Shengli, “The Challenges of Building Scalable Mobile Underwater Wireless Sensor Networks for Aquatic Applications”, IEEE Network, Special Issue on Wireless Sensor Networking, 2006. (doi:10.1109/MNET.2006.1637927)

[10] A. Muhammad, A. Mohd Rizal and Y. Abid, “Execution of Reed Solomon Coding as Forward Error Correction in Underwater Acoustic Communication", 2008.

[11] Q. Gang, X. Siyu and Z. Feng, “A Multi-User Detection Scheme Based on Polar Code Construction in Downlink Underwater Acoustic OFDM Communication System”, IEEE Access, vol.7, 2019. (doi:10.1109/ACCESS.2019.2916995)

[12] B. Anand V. and B. Mudit R., “Generations of Mobile Wireless Technology: A Survey”, International Journal of Computer Applications, vol.5, no.4, 2010.

[13] S. Milica, and B. Pierre-Philippe J., “Acoustic Communication”, 2013. (doi: 10.1007/978-3-319-16649-0_15)

[14] L. Lars, “On Shannon and ‘Shannon’s Formula.’”, Telektronikk 98, no.1, p.20–29, 2002.

[15] H. Thomas J. and Y. Tsih C., “Underwater Acoustic Communication Channel Capacity: A Simulation Study”, AIP Conference Proceedings, vol.728, p.114-121, 2004. (doi:10.1063/1.1843004)

[16] MathWorks MATLAB®, “Xilinx System Generator for DSP”, https://www.mathworks.com/products/connections/product_detail/xilinx-system-generator-for-dsp.html

[17] MathWorks MATLAB®, Help Center, "comm.Scrambler", https://www.mathworks.com/help/comm/ref/comm.scrambler-system-object.html

[18] X. Julio Diogo Miranda, "Modulation Analysis for an Underwater Communication Channel", M.Sc. thesis, Faculty of Engineering of the University of Porto, Porto, Portugal, 2012.

[19] MCC Support, Final Report of 3GPP TSG RAN WG1 #87 v1.0.0, Feb 2017. [Online].Available: http://www.3gpp.org/ftp/tsg_ran/WG1_ RL1/TSGR1_88/Docs/R1-1701552.zip (p.139)

[20] A. Erdal, "Channel Polarization: A Method for Constructing Capacity-Achieving Codes for Symmetric Binary-Input Memoryless Channels", IEEE Transactions on Information Theory, vol.55, no.7, 2009. (doi:10.1109/TIT.2009.2021379)

[21] L. Marco and R. Ruggero, "Carrier Frequency Recovery in All-Digital Modems for Burst-Mode Transmissions", IEEE Transactions on Communications, vol.43, no.2/3/4, 1995.

[22] S. Milica, "On the Relationship Between Capacity and Distance in an Underwater Acoustic Communication Channel", WUWNet'06: Proc. Of the 1st ACM International Workshop on Underwater Networks, pp.41-47, 2006.

[23] G. Alain, C. Pierre Y. and P. Annie, "Orthogonal Frequency Division Multiplexing with BFSK Modulation in Frequency Selective Rayleigh and Rician Fading Channels", IEEE Transactions on Communications, vol.42, no.2/3/4, 1994.

[24] H. Jianguo, S. Jing, H. Chengbing, S. Xiaohong and Z. Qunfei, "High-Speed Underwater Acoustic Communication Based on OFDM", IEEE International Symposium on Microwave, Antenna, Propagation and EMC Technologies for Wireless Communications Proceedings, 2005.

[25] Waves, “Physical radio channel models”, https://www.waves.intec.ugent.be/research/propagation/physical-radio-channel-models

[26] A. Michael A. and M. James G., “A simplified formula for viscous and chemical absorption in sea water”, Journal of the Acoustical Society of America, vol.103, 1998.

[27] T. Scott R., “Sound Propagation Considerations For a Deep-Ocean Acoustic Network”, M.Sc. thesis, Naval Postgraduate School, Monterey, California, 2009.

[28] G. Gökhan M. and Y. A. Özgür, “A General Framework for Optimum Iterative Blockwise Equalization of Single Carrier MIMO Systems and Asymptotic Performance Analysis”, IEEE Transactions on Communications, 61(2), 609–619, 2013.

[29] B. Valerio, C. Carlo and L. Ingmar, “Design of Polar Codes in 5G New Radio”, IEEE Communications Surveys & Tutorials, 2018. (doi:10.1109/COMST.2020.2967127)

# APPENDIX A

VHDL Code For Guard Band Generation:

```
library ieee;
use ieee.std_logic_1164.all;
use ieee.numeric_std.all;

entity GuardGenerate is
   port (
      Rst              : in std_logic;
      Clk              : in std_logic;
      CE               : in std_logic;
      Create           : in std_logic;
      Wait1ms          : out std_logic
   );
end GuardGenerate;

architecture GuardGenerate of GuardGenerate is

   signal Wait_r         : std_logic;
   signal bitRateCounter   : unsigned(19 downto 0);

begin

   process(Clk, Rst)
   begin
      if (Rst = '1') then
         Wait_r <= '0';
         bitRateCounter <= to_unsigned(0, bitRateCounter'length);
      elsif rising_edge(Clk) then
         if (CE = '1' and Create = '1') then
            Wait_r <='1';
         end if;
         if ( Wait_r = '1' and bitRateCounter <256000) then
            bitRateCounter <= bitRateCounter + 1;

         elsif (bitRateCounter > 256000 or bitRateCounter =256000 ) then
            Wait_r <='0';
            bitRateCounter <= to_unsigned(0, bitRateCounter'length);
         end if;
      end if;
   end process;

   Wait1ms <= Wait_r;

end Behavioral;
```

MATLAB Code For Guard Band Generation:

```
function GuardGenerate (this_block)


  this_block.setTopLevelLanguage('VHDL');

  this_block.setEntityName('SinCreate');

  this_block.tagAsCombinational;

  this_block.addSimulinkInport('Rst');
  this_block.addSimulinkInport('Create');

  this_block.addSimulinkOutport('Wait1ms');

  Wait1ms_port = this_block.port('Wait1ms');
  Wait1ms_port.setType('UFix_1_0');
  Wait1ms_port.useHDLVector(false);

  if (this_block.inputTypesKnown)
    if (this_block.port('Rst').width ~= 1)
      this_block.setError('Input data type for port "Rst" must have width=1.');
    end

    this_block.port('Rst').useHDLVector(false);

    if (this_block.port('Create').width ~= 1)
      this_block.setError('Input data type for port "Create" must have width=1.');
    end

    this_block.port('Create').useHDLVector(false);

  end  % if(inputTypesKnown)
   if (this_block.inputRatesKnown)
     setup_as_single_rate(this_block,'Clk','CE')
   end  % if(inputRatesKnown)

    uniqueInputRates = unique(this_block.getInputRates);

  this_block.addFile('SinCreate.vhd');

return;


function setup_as_single_rate(block,clkname,cename)
  inputRates = block.inputRates;
  uniqueInputRates = unique(inputRates);
  if (length(uniqueInputRates)==1 && uniqueInputRates(1)==Inf)
    block.addError('The inputs to this block cannot all be constant.');
```

```
  return;
end
if (uniqueInputRates(end) == Inf)
   hasConstantInput = true;
   uniqueInputRates = uniqueInputRates(1:end-1);
end
if (length(uniqueInputRates) ~= 1)
  block.addError('The inputs to this block must run at a single rate.');
  return;
end
theInputRate = uniqueInputRates(1);
for i = 1:block.numSimulinkOutports
   block.outport(i).setRate(theInputRate);
end
block.addClkCEPair(clkname,cename,theInputRate);
return;
```